



Groundwater recharge to a structurally complex aquifer system on the island of Tobago (Republic of Trinidad and Tobago)

David F. Boutt¹ · Marsha Allen¹ · Mark Settembrino¹ · Amber Bonarigo¹ · Joseph Ingari² · Rose Demars² · Lee Ann Munk³

Received: 11 September 2019 / Accepted: 7 December 2020 / Published online: 28 January 2021
© Springer-Verlag GmbH Germany, part of Springer Nature 2021

Abstract

Trinidad and Tobago is a developing two-island nation in the Lesser Antilles of the Caribbean. Tobago is the smaller island and has small highly heterogeneous aquifers composed of igneous and metamorphic crystalline rock with strong structural controls on the spatial distribution of permeability. Hydrogeologic analyses of the water budget and groundwater production suggest that portions of the island are underlain by prolific fractured-rock aquifer systems. This study quantifies the amount and spatial distribution of recharge, as well as the fraction of recharge captured by groundwater pumping, using historical data, new field data, remote sensing data, multiple storage quantification methods and stable isotope analysis. Despite extensive freshwater withdrawals, groundwater production reaches only ~10% of annual groundwater recharge. Groundwater capture zones are created using a first-order hydrologic balance approach and with backward particle tracking in a steady-state groundwater model. Both approaches to generating capture zones suggest that many wells capture water from outside their topographic watershed. The location of sustainable, high yield, fresh potable groundwater wells less than 1 km from the coast, that have fractured bedrock intakes well below sea level, supports the concept of a rigorous and active groundwater flow system. Understanding the hydrogeology of small bedrock island aquifers is critical to evaluating groundwater resources, especially in the Caribbean where there is strong seasonality in precipitation, finite surface-water storage and increases in potable water demand.

Keywords Fractured rocks · Groundwater management · Island hydrology · Trinidad and Tobago · Inter-basin groundwater flow

Introduction

Many island nations across the world are finding their water resources impacted by population growth, climate change, and sea level rise (Ferguson and Gleeson 2012; Karmalkar et al. 2013; Holding et al. 2016; Karnauskas et al. 2016). Groundwater supplies on islands are an important reserve of freshwater, but the hydrogeologic setting, geologic complexity, potential for salt-water intrusion, and minimal

groundwater storage make these resources difficult to use or access (Ferguson and Gleeson 2012; Kim et al. 2003; Banerjee et al. 2012). The geologic history of an island (carbonate reef/atoll, volcanic, clastic sedimentary) exerts a first-order control on the nature of the groundwater flow system (Charlier et al. 2011; Kim et al. 2003; Banerjee et al. 2012; Collins III and Easley 1999; Koh et al. 2006; Heilweil et al. 2012)—for example, islands with relatively uncomplicated geology and distribution of hydraulic conductivity have a well-developed freshwater lens, the size and extent being determined by climate and island topography (Collins III and Easley 1999; Banerjee et al. 2012; Schneider and Kruse 2003). Volcanic islands that are dominated by basalt flows have complicated distributions of hydraulic conductivity and flow systems that are strongly impacted by the presence of lava flows and intrusive dykes (Charlier et al. 2011; Kim et al. 2003; Koh et al. 2006; Hamm et al. 2005). Carbonate reef island systems have complex distributions of hydraulic conductivity due to secondary porosity development through karstification and carbonate stratigraphy (Stringfield et al.

✉ David F. Boutt
dboutt@geo.umass.edu

¹ University of Massachusetts, Amherst, 627 North Pleasant Street, 233 Morrill Science Center, Amherst, MA 01003-9297, USA

² Groundwater Resources International, PO Box 88, North Sandwich, NH 03259, USA

³ Department of Geological Sciences, University of Alaska-Anchorage, Anchorage, AK, USA

1979; Schneider and Kruse 2003; Banerjee et al. 2012). Islands comprised dominantly of igneous and crystalline metamorphic rocks, have low primary porosity and hydraulic conductivity, and these islands rely on fracturing and faulting to allow enhanced groundwater storage and flow system development. The preferential nature of the porosity and hydraulic conductivity distribution of this type of geologic setting impacts how water is stored and transported, leading to many questions regarding (1) volume of water stored, (2) water residence time distribution, and (3) sustainability of the resource. The quantification of recharge to such aquifer systems and discharge to wells and surface-water bodies is further complicated by the localized nature of the porosity and permeability.

Many decades of work have focused on continental hydrogeology of fractured rock aquifer systems (Davis and Turk 1964; Robinson and Beven 1983; Gustafson and Krásný 1994; Barton et al. 1995; Hsieh and Shapiro 1996; Brown and Bruhn 1998; Pyrak-Nolte and Morris 2000; Morin and Savage 2003; Min et al. 2004; Ohman et al. 2005; Boutt et al. 2010; Manda et al. 2013; Earnest and Boutt 2014). Complex structural and tectonic histories lead to the formation of multiple faults and fracture sets with complex spatial distributions (Gustafson and Krásný 1994; Caine et al. 1996; Caine and Tomusiak 2003; Banks et al. 2009; Biryukov and Kuchuk 2012). These processes along with the interaction between different scales of brittle and structural deformation give rise to distributions of hydraulic conductivity dominated by larger and more connected fracture sets. Structural elements associated with brittle faults and ductile shear zones have been shown to both increase and decrease permeability relative to the matrix (Caine et al. 1996; Caine and Tomusiak 2003; Bense et al. 2013; Williams et al. 2013). Strong depth dependence of smaller-scale fracture sets (Boutt et al. 2010) leads to depth-dependent permeability associated with fracture closure and fracture absence. Extensive field studies have shown that fractures that are well connected and oriented can increase the permeability by many orders of magnitude even at kilometer scales (Earnest and Boutt 2014; Barton et al. 1995; Bense et al. 2013). The presence of unconsolidated overburden, glacial sediments, colluvium, and saprolite has been shown to have different impacts on the underlying groundwater system development, but in almost all cases serve to be a source of storage and potential recharge to the fractured bedrock (Kretzschmar et al. 1994; Mogaji et al. 2011). Few studies have been able to focus on the groundwater system development of aquifers in an oceanic island setting, where the water budget and lateral boundaries are relatively well constrained (Kim et al. 2003; Banerjee et al. 2012; Collins III and Easley 1999; Koh et al. 2006; Heilweil et al. 2012).

This report documents the hydrogeologic conditions of the groundwater system on an island dominated by fractured igneous and metamorphic rocks. The island of Tobago is a developing island nation in the southeast Caribbean, whose

groundwater resources are strained, because the demand has doubled over the past decade (Mimura et al. 2007; Herrera et al. 2018). The island has a tropical climate where precipitation is strongly seasonal, during the dry season (January to May) its sole surface-water reservoir becomes exhausted, and groundwater serves as its main water resource. The majority of the island is composed of metamorphic and igneous rocks that have low matrix storage and permeability. Previous water supply investigations by the country's water management company (The Trinidad and Tobago Water and Sewage Authority-Water Resource Authority (WASA-WRA) suggest that the faulted and fractured bedrock serves as one attribute to enhance the permeability of the island. Due to increased pressure on surface-water resources, it is essential to increase understanding of the timing, amount, and spatial distribution of groundwater recharge to Tobago's aquifer systems to determine whether it is able to serve as a sustainable water source. Therefore, the objectives of this work are to (1) determine the overall water budget of the island, (2) assess the magnitude and timing of groundwater recharge, and (3) simulate the fate of the groundwater recharge to assess the volume of pumped groundwater to the water budget of the island in a structurally complex fractured aquifer system.

Background

Study site

The islands of Trinidad and Tobago are located in the Lesser Antilles in the southeastern Caribbean (Fig. 1). Tobago is the smaller of the two islands, located northeast of Trinidad with an area of 300 km², and highest elevation of ~580 m above sea level. Structurally, Tobago is situated on the northeastern corner of the South American continental shelf (Speed et al. 1993; Speed and Horowitz 1998). It is approximately 41 km in length and 10 km in width at its widest point, oriented southwest to northeast. Trinidad and Tobago is a developing country with a population of approximately 1.365 million as of 2016 according to The World Bank. The local water management agency has noted that the current water resource is challenged by the impacts of climate change, pollution, industrial demands, flooding, degrading wetlands, watersheds and coastlines, growing population and degrading infrastructure (Government of the Republic of Trinidad and Tobago 2017).

Hydrology of the island

Atlantic trade winds predominantly flow from the east/northeast, and there are two distinct seasons in this region with 1-year cycles: a dry season lasting from January to May and a wet season from June to December. During the wet season, the trade winds are intercepted by the main mountain

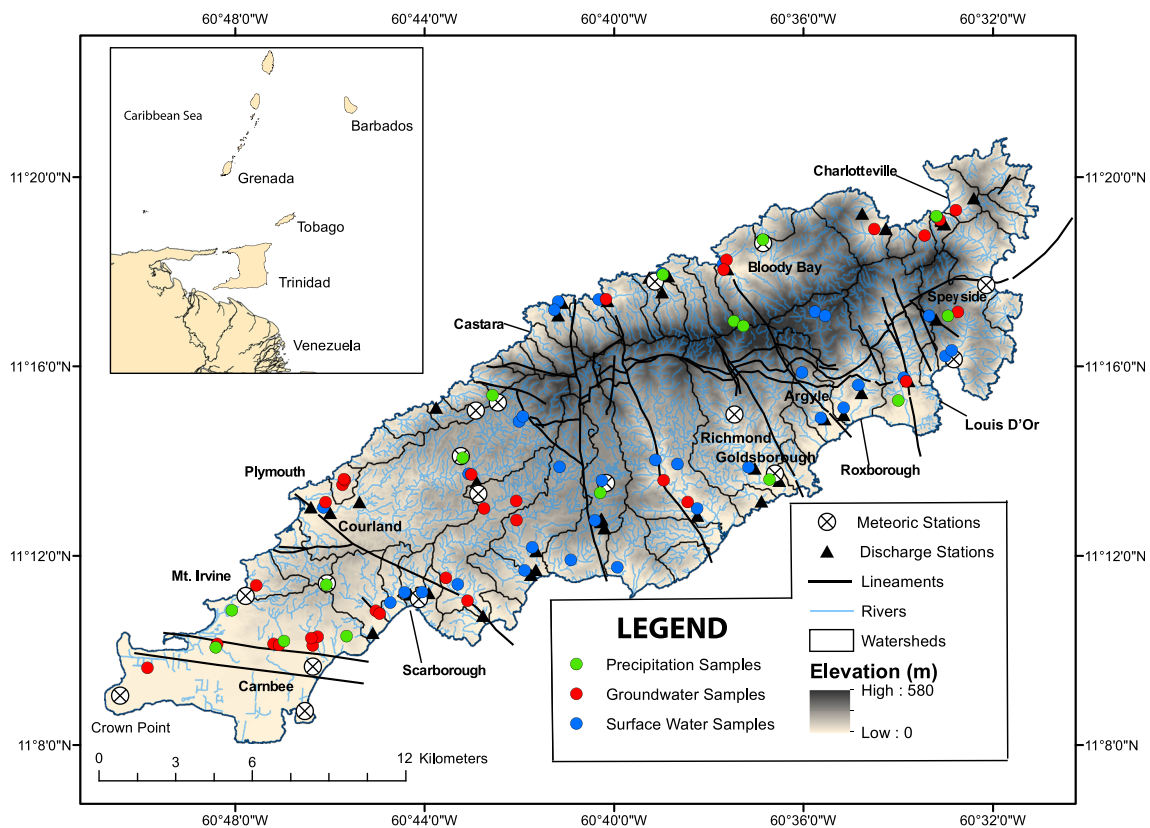


Fig. 1 Map of Tobago, West Indies, with inset map showing geographical location relative to surrounding countries. Watershed boundaries are from a 25-m digital elevation model (DEM). Illustrated faults and structures illustrated are acquired from Snoke et al. (2001)

ridge (580 m) on the island creating an orographic effect leading to increased precipitation. Precipitation reaches a maximum in November (~300 mm) and a minimum in March (~40 mm). Mean annual rainfall on Tobago is 1,900 mm. Evapotranspiration (ET) dominates the terrestrial water budget of the island with ET rates exceeding ~1,200 mm/year. The island has numerous rivers and streams, of which all are perennial. Dry season flows, while low, are assumed to be sustained by baseflow via groundwater discharge. Major watersheds are delineated in Fig. 1, with the largest of these being Courland, Bloody Bay, Goldsborough, Richmond, Louis D'or, and Argyle.

Geology, structure, and hydrogeology of Tobago

The island of Tobago has experienced multiple tectonic events over time due to its location within the Caribbean Plate/South American Plate transition boundary (Aitken et al. 2011, Snoke et al. 2001; Speed et al. 1993; Speed and Smith-Horowitz 1998). Previous studies suggest the island, which is predominantly comprised of Mesozoic Age rocks, was deformed and transported tectonically northeast over time (Snoke et al. 2001).

The lithology and geological features of Tobago are documented in studies conducted by Speed and Smith-Horowitz

1998 and Snoke et al. 2001 (Fig. 2). Snoke et al. 2001 contains a detailed geologic map and cross-sections from the island geology. The bedrock of the island of Tobago comprises primarily of Mesozoic plutonic rocks and volcanic rocks with minor Tertiary Age platform limestone, conglomerates, clays and marls (Snoke et al. 2001). The island is composed of three main east–west striking lithologic belts: The North Coast Schist, the Tobago Volcanic Group, and a Plutonic Suite. A mafic dike swarm intruded the Tobago Volcanic Group and Plutonic Suite, whereas the North Coast Schist contains only a few scattered post-metamorphic dikes. On the southeastern end of the island there is a Quaternary coralline limestone platform composed of unconsolidated marine deposits (the Rockly Bay Formation; Snoke et al. 2001). It includes clays, sandy clays, ferruginous silts, sands, marls, pebble beds and conglomerate with clay predominant in the upper sections and sands and pebble beds predominant in the lower sections. The formation reaches depths of about 190 m in the southern sections of the island.

The North Coast Schist is the northernmost lithologic unit on the island and is estimated to have formed in the Early Cretaceous (Snoke et al. 2001). The majority of the unit is low-grade greenschist-facies. The Tobago Plutonic Suite is a heterogeneous intrusive igneous complex, which intruded and metamorphosed both the North Coast Schist and the Tobago

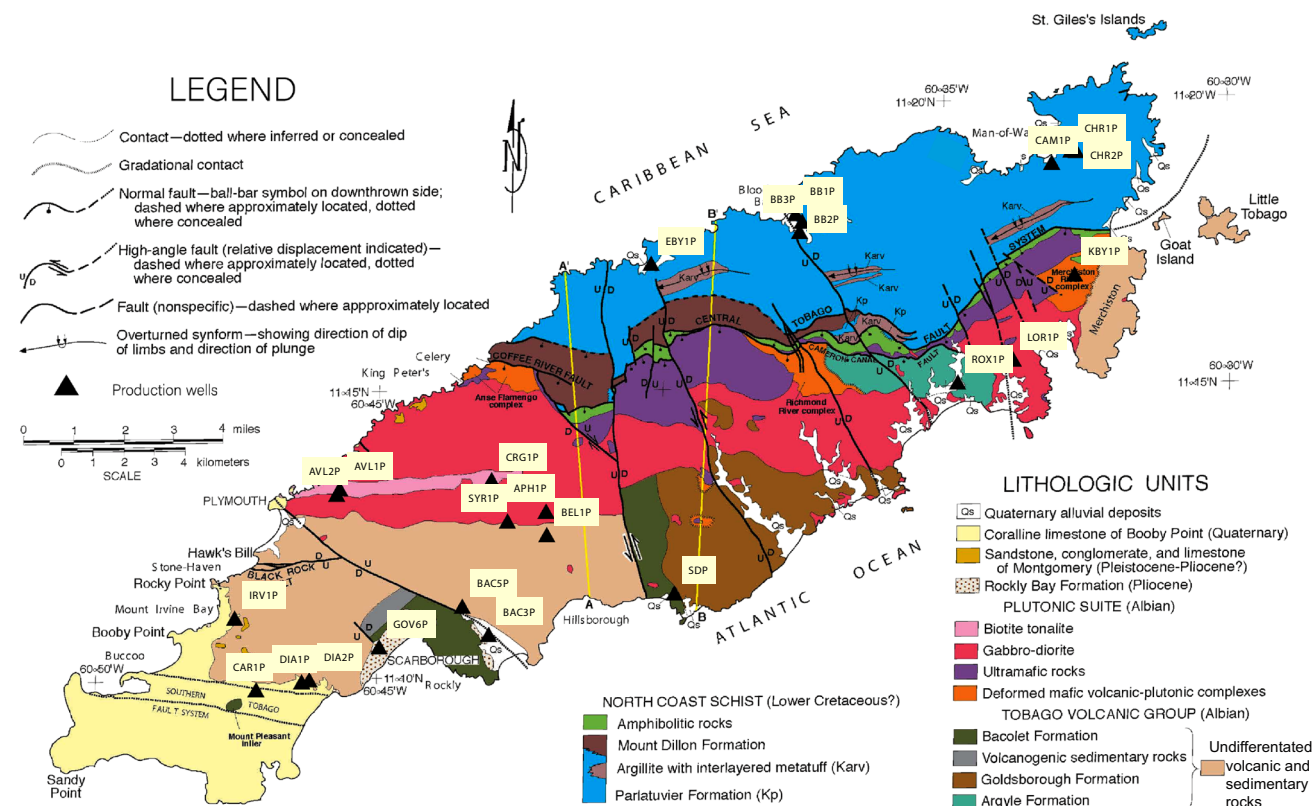


Fig. 2 Modified geological map of Tobago, West Indies, from Snoke et al. (2001), illustrating faults and structural features, lithological units, and production well locations

Volcanic Group. The Tobago Volcanic Group caps the intrusive Plutonic Suite and is the southernmost lithologic band on the island. The Volcanic Group consists mainly of mafic volcanoclastic breccias. The Plutonic Suite occurs through various erosional windows, and it appears that The Tobago Volcanic Group thins eastward as it approaches the Plutonic Suite. A mafic dike swarm intruded the Plutonic Suite as well as the Tobago Volcanic Group.

Due to the island's location near the Caribbean Plate/South American Plate Boundary transition zone and its affiliation with island arc complexes associated with the Caribbean Plate subduction zone, it has experienced numerous episodic deformational events. Most of the island's major faults are generally oriented N–S to NW–SE for the Southern Tobago Fault System which is oriented W–E. The Mesozoic tectonic activity created penetrative plastic deformation coupled with green schist facies metamorphism observed in the amphibole aureole and North Coast Schist (Snoke et al. 2001). This led to the subsequent alignment of foliation and associated lineation with geologic contacts (Snoke et al. 2001). Faults and fractures associated with these structures introduce heterogeneity into the aquifer system that may create preferential flow paths that cross topographic watershed boundaries and allow for exceptional groundwater

production rates (Caine and Tomusiak 2003). A thick saprolite layer is located between the above soil deposits and the fractured bedrock. Saprolite thicknesses in tropical climates are approximately 1–8 m in depth (Buss et al. 2008, 2010; Pett-Ridge JC et al. 2009).

The island does not have extensive porous media aquifers (Hydrogeological Atlas of the Caribbean Islands and UNESCO 1986). The Rockly Bay and similar formations can contain moderate amounts of groundwater which is stored and transmitted through permeable sand and gravel, which provide groundwater recharge to underlying bedrock fracture systems. Several low to moderate yield wells are installed in this formation. However, its limited lateral extent and high clay content restrict the amount of groundwater, which can be extracted from this unit over the long term. The Quaternary limestone in the lowland area of the island averages about 12 m in thickness. Its secondary permeability can be high; however, because it is thin and has a unit base elevation extending only 10 m below sea level, it is very limited in its usefulness as a sustainable public water supply source. Its primary hydrologic function is as a source of surface recharge to underlying formations. Production wells targeted in the underlying igneous and metamorphic bedrock suggest that these units are capable of producing significant amounts of freshwater.

Materials, methods, and study approach

The following sections detail the methods of this integrated hydrologic, isotopic, and groundwater modeling study. The study first derives a complete hydrological budget of the island using historical meteorological and hydrologic data. These water budget components are used to determine the spatial and temporal variation of groundwater recharge on the island. The total annual groundwater recharge is then used as input into a steady-state groundwater flow model to assess the capture amount of groundwater production wells on the island on an annual basis. Finally, the isotopic characterization assists with corroborating physical hydrological conceptualizations.

Water balance components

Hydrologic data from observations provided by WASA-WRA (See supplemental materials) and models are used construct a water budget for the island of Tobago consisting of three main components: precipitation, evapotranspiration, and stream discharge. Island-scale estimates of mean annual precipitation and evapotranspiration are presented at a 25 m scale, and watershed-scale annual-stream-discharge estimates. Together these components are used to calculate annual groundwater recharge rates across the island. The calculation of the spatially distributed groundwater annual recharge rates serves two main purposes—first, they are used as the input for a process-based groundwater flow model; secondly, the recharge rates are compared to existing groundwater extraction wells to determine the current volume of groundwater tapped by wells. Finally, monthly estimates of precipitation and evapotranspiration are used to explore seasonal patterns in the water budget and compare with stream discharge observations but are not used in the subsequent groundwater model described.

Precipitation

A 50-year record of daily precipitation data from 16 rain gauge stations provided by WASA-WRA is used to generate spatially distributed average monthly and annual isohyetal maps for the island of Tobago (Fig. 1). The historical precipitation data was incomplete, and therefore monthly averages for each of the 16 stations were calculated from the most complete records (>95% complete) for the greatest number of stations (years 1974–2006; Table S1 of electronic supplementary material *ESM1*). To interpolate between rain gauge stations, a log-elevation weight is applied for each monthly coverage based on a regression analysis of elevation and precipitation using stations least likely impacted by rain shadow events. A review of precipitation records revealed that a log relationship was best fitting to model precipitation with

elevation, which is supported by (Daly et al. 1994; Fig. S1 of *ESM1*).

The best and simplest fit was represented by the equation:

$$P = A \times \ln(0.3048z) + C \quad (1)$$

where P is monthly precipitation (mm/year), A is a dimensionless scaling term, z is the topographic elevation (m) above sea level, and each monthly value of C is an intercept value corresponding to an optimized R^2 value fit for the most reliable stations (Table S2 of *ESM1*). The value of A was 20 for all months except during the dry season, specifically February to April where more modest increases in precipitation with elevation were represented by value of 7 for A .

In order to accommodate higher estimated precipitation values at elevations beyond the highest available measurement station, a linear multiplier was used for elevations greater than 244 m using the following equation:

$$P = 1.53z \quad (2)$$

The mean annual precipitation (mm/year) distribution was created using an inversely weighted distance interpolation of measured rain gage location values averaged with precipitation values from the elevation models. This approach is the simplest way to incorporate the nuances of potential rain shadow effects recorded by each station location data, while allowing precipitation/elevation relationships to be used as a more transferable predictor across the island. While elevation is the primary dependent variable, the coverage of the existing meteorological stations allowed robust predictions to be determined.

Maps of monthly and annual precipitation were calculated by applying the equations above to a 25 m digital elevation model (DEM) of the island to produce spatially distributed precipitation values. These values represent long-term average quantities (~50 years) suitable for water budget assessments at the watershed scale.

Evapotranspiration

Evapotranspiration is estimated using a combined station and modeling approach. There is only one complete meteorological station on Tobago (Crown Point Airport) that records data relevant for the calculation of evapotranspiration (ET) operated by WASA-WRA. The Crown Point Airport is located in the far southwest corner of the island (Fig. 1), a lowland area with developed urban and agricultural land use, and likely not representative of ET conditions island wide. Monthly potential evapotranspiration (PET) estimates are compiled from satellite data and the Hargraves method (Hargreaves and Allen 2003).

The CGIAR-CSI Global-PET Database (Zomer et al. 2008) offers a feasible approach to accurately model PET

without the uncertainty produced from underconstrained linear interpolations. The CGIAR PET model incorporates the Hargreaves PET method and the World Global Climate Data (Zomer et al. 2008) input parameters from SRTM topographic data and high-resolution climate observations to produce PET estimates at a 95-m grid scale. Monthly average PET (mm/month) geo-datasets of mean temperature (T_{mean} , C°), daily temperature range (TD, C°), and extraterrestrial radiation (RA; radiation on top of atmosphere expressed in mm/month as equivalent of evaporation), are combined using the following equation according to the Hargreaves method (Hargreaves and Allen 2003):

$$\text{PET} = 0.0023 \times \text{RA} \times (T_{\text{mean}} + 17.8) \times \text{TD}^{0.5} \quad (3)$$

Following the Food and Agriculture Organization application of the Penman-Monteith equation, annual actual evapotranspiration (AET) estimates are then derived from a monthly mean PET value to distinguish between seasonal changes in available water (precipitation) and PET (Allen et al. 1998). This analysis yields an AET estimate of 76% of PET and is used in the further water balance calculations. As with the precipitation product above, annual and monthly raster products of actual evapotranspiration are produced at the 25-m scale for the whole island.

Stream discharge

In this study, stream discharge is estimated from observations to provide a product at the watershed scale that is used to calculate in-place groundwater recharge. Stream discharge estimates for Tobago were produced using a combination of WASA-WRA historical field data and the field measurements taken in 2014 as part of this study (black triangles in Fig. 1). They are incorporated into an adjusted rational method to model mean annual stream discharge conditions for the island (Arenas 1983). The rational method predicts streamflow discharge by integrating precipitation and watershed area by a coefficient (Dingman 2002). Due to the data limitations and extreme nature of precipitation and stream discharge in Tobago, a more comprehensive time-series analysis was forgone in lieu of this adjusted rational method. High stream flow values remain uncertain, and it is generally assumed that most peak rainfall events contribute entirely to stream discharge (Arenas 1983).

Stream discharge coverages were estimated as an annual streamflow per basin (mm/year). Mean annual discharge by basin was estimated using a modification of the rational method approach (Dingman 2002). Land cover data (Fig. S2 of ESM1) was obtained for the island (Baban et al. 2009) and the following was assigned streamflow discharge coefficients: forest = 10, agricultural = 30, urban = 80, water = 100 (Dingman 2002). An island-wide map of percent slope was

also calculated using a 25-m DEM. Due to the high abundance of steep slopes on the island and the coarse nature of the DEM, a threshold of 60% slope or greater was used to model a 100% stream discharge rate. Remaining slope values were assigned streamflow discharge coefficient values based on a 1–100 scale (with 60% slope being 100). Final discharge calculations were made using an assumption that 60% of precipitation falls during light-moderate intensity rain events during times when PET and soil infiltration rates are high enough to negate a direct contribution to streamflow. Equation 4 shows this discharge calculation:

$$Q = \left[\frac{\text{SLP} + \text{LC}}{2} \right] 0.4 P \times A \quad (4)$$

where Q is stream discharge (m^3/s), SLP and LC are slope and landcover (both dimensionless), P is annual precipitation in mm/year, and A is watershed area (m^2). The remaining 40% of moderate to high intensity rain events directly contribute to potential streamflow and according to the streamflow coefficient assigned to a raster grid (of the same dimensions as the DEM, 25 m). The final streamflow coefficient for each raster grid cell is the result of an equally weighted slope and land cover characteristic. The Courland basin remained an exception in that it has anomalously low measured discharge values, likely due to the transfer of surface water to the Hillsboro Dam. In order to accommodate this data, a manual value was assigned to the basin to agree with the mean annual stream discharge measured.

To explore the seasonality of the water budget and to provide a calibration target for the groundwater flow model, estimates watershed-scale dry season discharge are provided, which should be predominantly groundwater discharge (Boutt et al. 2001). Stream discharge data from 23 stations (WASA-WRA) with records of repeated measurements across multiple years provided direct values for the watersheds in which they were located. Stream discharge rates Q_w , m^3/s , for the remaining watersheds are calculated using a watershed scaling (Eq. 5) to extrapolate the measurements to basins with erratic data records or to those that were not sampled at all but are in close proximity to discharge sample locations:

$$Q = 5.5E-9 (A) + 0.00042 \quad (5)$$

Dry season discharge values were the result of known values, watershed area, and manual fitting of watersheds in close proximity (for example, small basins on the northern coast were manually assigned values based on bordering watersheds of similar size).

Groundwater recharge from water budget analysis

To estimate mean annual groundwater recharge, groundwater recharge units (discrete subwatershed classifications) were

delineated using a 25-m DEM. Recharge for each groundwater recharge unit (GRU) was calculated in ArcGIS using the water balance approach with the mean annual maps of precipitation, streamflow, and evapotranspiration (Fig. S3 of ESM1). Individual raster datasets of precipitation and streamflow at 25 m and evapotranspiration at 95 m were summed over the groundwater recharge unit area to provide the basis for the calculation. The water balance approach relates recharge to streamflow, evapotranspiration, and precipitation using the arithmetic equation:

$$\text{Potential Recharge} = \text{Precipitation} - \text{Streamflow} - \text{AET} \quad (6)$$

At individual meteorological stations (Fig. 1) monthly site-specific recharge estimates are presented using the monthly precipitation and evapotranspiration products with the corresponding wet or dry season stream discharge estimates for the encompassing basin. These seasonal recharge estimates are only used to characterize seasonality in recharge and are not used in the steady-state groundwater flow model.

Stable isotopic composition of precipitation, surface water, and groundwater

Analysis of stable isotopes of water across the island is used to identify water sources. In March and December 2014 samples were taken from 32 groundwater wells, 36 streams, and 5 springs throughout the island of Tobago. In addition, 8 months of precipitation samples (June 2014 – January 2015) from 11 meteoric stations on the island were also collected. In the summer of 2015 groundwater samples were taken from 8 newly drill test wells (see Fig. 1 for locations of all water samples).

Samples were collected in March and December 2014 and were analyzed at the Stable Isotope Laboratory at the University of Massachusetts. All water samples were filtered and placed into 2-ml glass auto-sampler vials with a polytetrafluoroethylene septa. The isotopic composition ($^2\text{H}-\text{H}_2\text{O}$, $^{18}\text{O}-\text{H}_2\text{O}$) of hydrogen and oxygen of the water molecule of surface water, springs, precipitation and ground water were measured by wavelength scanned cavity ring-down spectrometry on unacidified samples by a Picarro L-1102i WS-CRDS analyzer (Picarro, Sunnyvale, CA). Samples were vaporized at 110 °C. A 5- μl Hamilton glass syringe draws 1 μl of sample to inject into a heated vaporizer port (110 °C). For each injection, the absorption spectra for each isotope are determined 20 times and averaged. Between injections, the needle is rinsed with 1-Methyl-2-pyrrolidinone and the sample chamber is flushed with dry nitrogen. To further eliminate memory effect between samples, each sample is injected six times and the results of the first three injections are discarded. In addition, the lab has adopted a modified version of the technique of Penna et al. (2012); samples are run in groups

in order of isotopic compositions and/or grouped by water source and location. Three standards that isotopically bracket the sample values are run alternately with the samples. Secondary lab reference waters (from Boulder, Colorado; Tallahassee, Florida; Amherst, Massachusetts) were calibrated with Greenland Ice Sheet Precipitation (GISP), Standard Light Antarctic Precipitation (SLAP) and Vienna Standard Mean Ocean Water (VSMOW) from the IAEA (Craig 1961). Results are calculated based on a rolling calibration so that each sample is determined by the three standards run closest in time to that of the sample. Long-term averages of internal laboratory standard analytical results yield excellent instrumental precision of 0.51‰ for $\delta^2\text{H}-\text{H}_2\text{O}$ and 0.08‰ for $\delta^{18}\text{O}-\text{H}_2\text{O}$. House waters analyzed from 2012 to 2017 show no drift or consistent offset in isotopic composition. The $\delta^{18}\text{O}$ of each sample is calculated using the following equation, where R is equal to $\delta^{18}\text{O} / \delta^{16}\text{O}$.

$$\delta^{18}\text{O}_{\text{sample}} = \left[\frac{R_{\text{sample}}}{R_{\text{VSMOW}}} - 1 \right] \times 10^3 \quad (7)$$

Annual weighted averages of $\delta^{18}\text{O}$ were calculated for each precipitation station using the volume of water measured in the rain gauge at the time each sample was collected (ESM2). To estimate the isotopic signature of precipitation that recharges groundwater at each precipitation station, the volume weighted averages were weighted again by the amount of precipitation resulting to possible recharge the aquifer monthly; herein referred to as recharge signatures. March and December 2014 surface water and groundwater samples are binned into dry and wet season samples to determine whether any seasonal dependence exists on the isotopic compositions. There was limited documentation of production well characteristics such as: well depths, screen depths, well logs. All available data is included in Table S2 of ESM2.

Production well contributing areas using a hydrologic balance approach

The analysis to estimate the contributing areas to groundwater pumping is executed using two different approaches. The homogeneous approach compared the 2013 average annual groundwater production rates for the island wells in a given GRU to annual groundwater recharge estimates to that GRU. Average annual pumping rates are used from 2013 in this analysis instead of long-term averages because groundwater pumping in Tobago is expected to increase dramatically in the future, and 2013 production rates are not only the most recent and reliable data available, but are also historically the highest rates of production on the island. If groundwater production is greater than the recharge to the GRU in which it is located, it is assumed that groundwater is being sourced from a larger contributing area. In this case, the annual production of a well is

distributed to the nearest topographically higher GRU(s) annual recharge, until the well's annual production rate has been matched by the accumulated annual recharge of the GRUs. This method assumes that all water captured by groundwater wells is captured within topographic surface water divides.

An additional and separate hydrologic balance is performed, which considers the possibility of faults influencing the direction of groundwater flow in crystalline rock aquifer systems. GIS shapefiles of faults produced by Snoke et al. 2001 (Fig. 2) are overlaid onto the GRU recharge coverage. The contributing area to groundwater pumping is estimated in a well field intersected by a structure; the same methodology as already mentioned was used, except along GRUs intersecting these structures.

If a well field's production rate exceeded that of its local GRU's annual recharge, its contributing area was extended up gradient along the main axis of the feature, taking note of which of the surrounding GRUs intersect the feature. The calculation continued until the number of GRUs necessary to meet the recharge needs of the production wells were achieved.

In those cases where it appeared that multiple well fields were accessing the same GRU, the GRUs are divided by the number of well fields and make up for the difference by selecting additional GRUs to satisfy the deficit. This process was repeated for all well fields and a map depicting the contributing GRUs to production wells was generated.

Steady-state groundwater flow model

A three-dimensional (3D) steady-state groundwater flow model for the island of Tobago was developed using the Newton formulation (NWT) of MODFLOW-2005 (Niswonger et al. 2011) with the upstream weighting package and the layer property flow package for flow calculations. The model is designed to simulate mean annual conditions and to (1) estimate the contributing areas of the production wells and (2) assess the water budget of the groundwater system. The model was constructed using a 200×200 -m horizontal grid with a six-layer vertical grid with variable thickness in the vertical dimensions for a total of $\sim 1.8 \times 10^5$ active cells. A 25-m-resolution DEM was converted to a triangular irregular networks (TIN) elevation coverage in groundwater modeling system (GMS) and interpolated into a MODFLOW finite-difference grid. The height or Z value for each cell was based on topographical data, which was interpolated based on the mean elevation for each grid cell, creating a representative 3D grid. The spatial dimensions of the model were chosen to allow appropriate representation of the model topography, at scales applicable to represent hydrogeologic features and flow paths and allow for mass-balance in the solution to be achieved. Vertical resolution was chosen to allow adequate definition of vertical components of flow paths and

representation of surficial geologic deposits. Water enters the model domain through recharge and leaves either through stream discharge, pumping wells, or submarine groundwater discharge. Mean annual recharge to the model is applied using the island-scale water budget analysis (from the aforementioned methods) with the MODFLOW Recharge (RCH) package to the upper most active model cell. Recharge to the model was directly incorporated from the preceding hydrological budget calculations and only adjusted to match total island recharge based on small differences in total island surface area caused by discretization. Recharge was not adjusted spatially in the model; therefore, any uncertainty or bias in recharge values is transferred to the hydraulic conductivity values, which were the only calibration parameters.

Specified head cells are set to sea-level (0 m) on the coast, thus representing the seaward model boundary as a vertical interface of constant head. This approach does not account for physics of freshwater/saltwater interactions but does allow fresh groundwater to exit the model at that boundary to simulate possible submarine groundwater discharge. Streams were simulated with the MODFLOW Stream (STR) package with a simplified river network to capture the largest of drainages (i.e. some small coastal streams and drains were omitted). Pumping wells and their screen locations and average annual production rates were modeled using the MODFLOW Well (WEL) package. Locations where hydraulic head observations and stream discharge are available are imported with MODFLOW Observations (OBS) package for model calibration and validation. The mean and standard deviation of hydraulic heads from observation wells were calculated over time periods ranging from 5 to 12 years. The observation data was divided into training and testing data sets using a 50–50 split. Initial hydraulic conductivities were assigned based on the surficial and bedrock geologic map (Fig. 2) through the correlation of aquifer testing data and adjusted in the calibration process. Available constant rate pumping tests are used to extract hydraulic information about the geologic formations the wells penetrate. Since the majority of the bedrock wells are targeted along significant geologic structures such as fractures, the estimates of hydraulic properties are considered estimates of the hydraulic properties of these structures in particular and not those of the background fracture network.

The performance of the steady-state model was evaluated by comparing observed and simulated hydraulic heads and simulated stream baseflow discharge to estimated dry season discharge values. Satisfactory models balanced the geographic distribution of residuals in hydraulic heads with small errors in simulated and observed values. Final model selection achieved the smallest compound residual error factoring in the hydraulic heads and discharge values.

Based on specific capacity analysis the average transmissivity for the Tobago bedrock wells is 6.19×10^2 m²/day (7.16×10^{-3} m²/s); the average hydraulic conductivity (K) is

9.9 m/day (1.14×10^{-4} m/s). Values of hydraulic conductivity ranged from 70 m/day in basaltic andesite to 0.03 m/day in the North Coast Schist. The average transmissivity for the Tobago overburden wells is 1.66×10^2 m²/day (2.92×10^{-3} m²/s), the average K is 32.8 m/day (3.8×10^{-4} m/s). In general, the bedrock wells are more transmissive than the overburden wells but when normalized for the equivalent aquifer thickness (b) the hydraulic conductivity of the overburden wells is larger than the bedrock by a factor of 3 (approximately 10 m/day compared to 33 m/day). The qualitative results of the hydrogeological performance of the island's aquifers suggested that the sand and gravel aquifers have high local hydraulic conductivity, but the limited thicknesses (and spatial extent) cannot provide the transmissivity needed for an island-wide water supply. The reported hydraulic conductivities are very high for most of the bedrock formations and indicate prolific aquifers. The hydraulic conductivity results for the bedrock wells indicate that the Tobago volcanic series (the basaltic andesite and undifferentiated units) have the highest hydraulic conductivities. The bedrock wells penetrating the North Coast Schist have the lowest hydraulic conductivities, and the wells located in the lowlands (the Booby Point formation) have some of the lowest hydraulic conductivities. These wells are screened within fine grain confining units and would likely have high storage but low transmissivity.

Depending on the thickness of surficial deposits, numerical model layers 1–3 encompass the surficial geologic units and shallow bedrock in areas outside of the surficial deposits. The rest of the model layers (4–6) are assigned the bedrock hydraulic conductivity and are homogeneous with depth. Bottom of model domain is set to be flat at 300 m below sea level, with average cell thickness of 50 m. The modeled hydrogeologic units and hydraulic properties were not adjusted at scales below the major mapped litho-stratigraphic units. Lineaments and their assigned hydraulic conductivities were applied to the model at the 200×200 m cell scale and treated as isotropic at the cell scale. Contributing areas to the production wells were determined by reverse particle tracking using MODPATH and then manually digitizing a polygon around the resulting generated path lines. Care is taken to capture the simulated path lines with a polygon that represents more than one simulated particle path.

Results

Island scale water balance and groundwater recharge estimates

The first rigorous analysis of the island of Tobago's hydrological budget is presented in (Table 1; Fig. 3) The annual average precipitation across Tobago is estimated to be 1,889 mm/year (Fig. 3a). Due to the

orographic effect on precipitation, the highest rates of mean annual precipitation correspond with the highest elevations in the central and northeastern regions of the island. Annual rates of rainfall in these regions range from 2,000 to 2,600 mm/year. The lowest rates of annual rainfall occur in the lowlands of the southwest region of Tobago, and in the northern region that is affected by the rain shadow, whereby annual rates of rainfall in these regions ranged from 960 mm/year to 1,800 mm/year.

Annual AET on Tobago is approximately 1,243 mm/year, and accounts for 66% of losses from annual precipitation. The spatial distribution of actual evapotranspiration is not highly variable over the island but does vary from a low value of 1,100 mm/year in the drier southwest to 1,320 mm/year in the wetter northeast (Fig. 3b). The monthly distribution of precipitation and evapotranspiration has implications for the timing of streamflow and groundwater recharge on the island. The highest PET values coincide with the lowest precipitation values in April and May; during those periods AET is 40% of PET (Fig. S4 of ESM1). During the highest rainfall month (November), PET is only moderate, leaving excess precipitation for stream discharge and recharge. This seasonal fluctuation in PET and rainfall reflects the temporal availability of water on the island.

The total island scale stream discharge rate for Tobago is estimated to be 256 mm/year. To test the validity of the stream discharge model, estimates are compared to historical annual average discharge measurements provided by The Trinidad and Tobago WASA-WRA at three major rivers throughout the island Bloody Bay (measured 0.22 m³/s, calculated 0.22 m³/s), Louis D'or (measured 0.20 m³/s, calculated 0.21 m³/s), and Richmond (measured 0.29 m³/s, calculated 0.30 m³/s; Fig. S5 of ESM1).

The island-scale water budget analysis estimated approximately 390 mm/year. (0.117 km³ – annually) of water enters the ground as recharge on the island. Recharge is strongly seasonal and dependent on evapotranspiration (Fig. S6 of ESM1). Almost all groundwater recharge occurs during a 7-month span from June through December, with maximum values across the island for most sites occurring during October and November. The largest rates of groundwater recharge occur in the highlands in central and northern Tobago, which is also where the highest rates of precipitation occur.

Values used for each component of this analysis represent the mean values and are not intended to represent conditions of extreme drought or heavy precipitation. Human withdrawals of water from surface and ground reservoirs are not accounted for in this budget and can have a large influence on stream discharge values used in this model.

Table 1 Annual water balance (mm/year) for the island of Tobago determined from geospatial analyses

Water budget component	Total (mm/year)	Dry season (mm/year)	Wet season (mm/year)
Precipitation	1,889	–	–
Actual evapotranspiration	1,243	–	–
Stream discharge	256	60	196
Recharge	390	–	–

Contributing area to production well: hydrologic balance approach

Table 2 presents the total well production and GRU recharge rates in cubic meters per year (m³/year). Using the recharge estimates, 11 out of the 14 well fields evaluated are recharged from areas beyond the local GRU. The Charlottesville (CHR1P and CHR2P), Englishman’s Bay (EBY1P), and Mount Irvine Bay (IRV1P) well fields are low producers and are currently withdrawing less water than is available for recharge within the local GRU. In contrast, the Bacolet (BAC1P, BAC3P, and BAC5P), Arnos Vale (AVL1P,

AVL2P), Craighall (CRG1P), and Government Farms (GOV6P) well field pump in excess of 500% of the local GRU recharge. These wells must be located in watersheds with large upgradient contributing areas or are located along major structures that enable groundwater flow on a regional scale.

Water balance calculations considering the additional contribution of water from up-topographic gradient GRUs, indicate that almost all of the well fields in current production are pumping less water than the available recharge within their topographic watershed. The two major exceptions to this are the wells that reside in the watersheds of Arnos Vale (AVL1P,

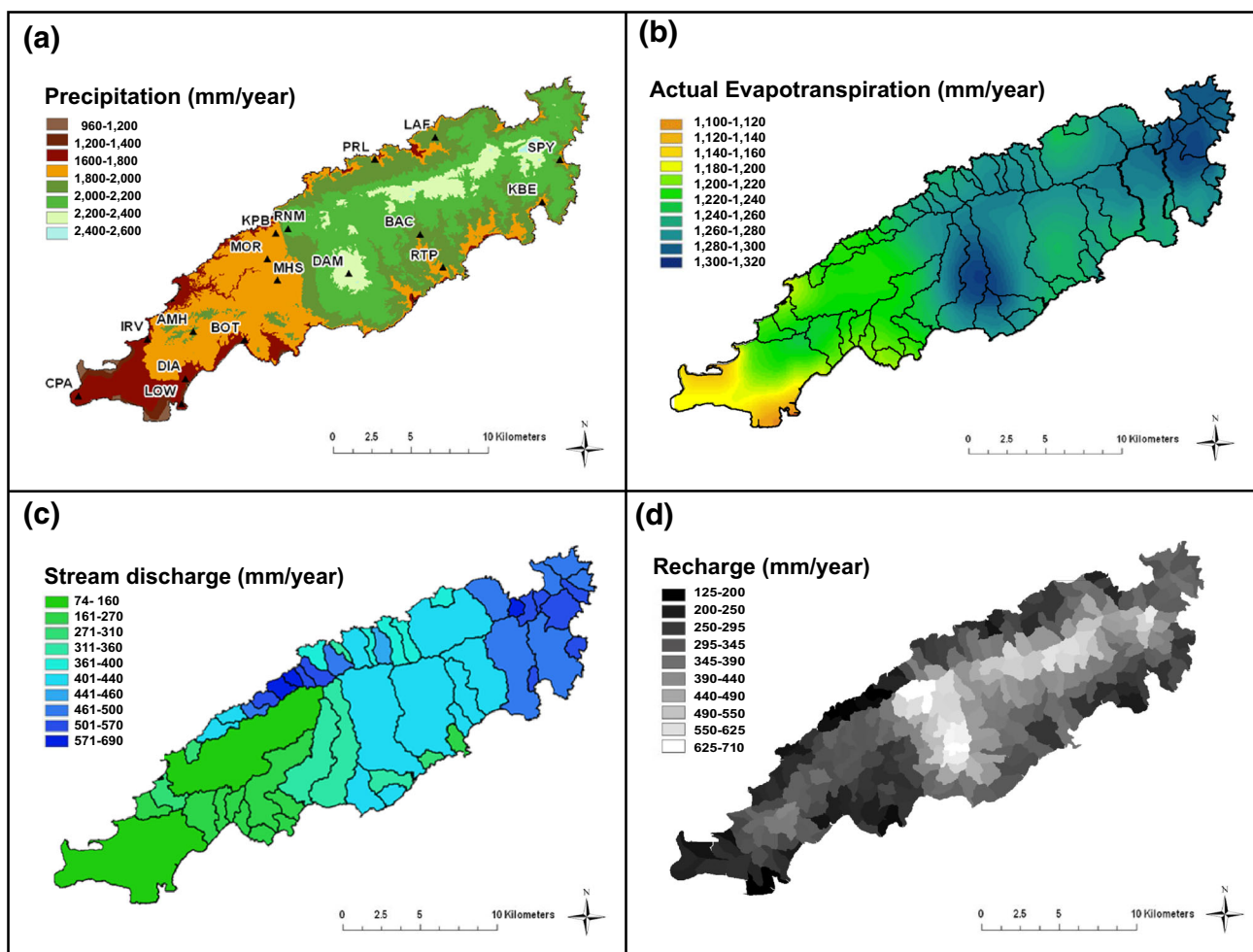


Fig. 3 Hydrological budget of Tobago: **a** precipitation; **b** evapotranspiration; **c** streamflow; **d** recharge. Groundwater budget calculation [precipitation – evapotranspiration – streamflow = change in storage (recharge)]

Table 2 Annual well production for major well fields compared to GRU recharge estimates

Common well name	Well ID	GRU No.	GRU area (km ²)	GRU recharge (m ³ /year)	2013 annual production (m ³ /year)	Production/GRU recharge (–)
Adelphi No. 1	APH1P	243	1.23	2.3E+05	3.3E+05	143%
Amos Vale Nos. 1 and 2	AVL1P	158	0.76	1.4E+05	1.1E+06	757%
Bacolet No. 5	BAC5P	91	0.86	1.3E+05	1.1E+06	855%
Bacolet No. 3	BAC3P	93	1.17	1.9E+05	9.6E+05	509%
Belmont No. 1	BEL1P	79	1.11	2.1E+05	4.6E+05	218%
Bloody Bay Nos. 1–3	BB1P	122	0.47	9.3E+04	3.4E+05	361%
Campbelton No. 1	CAM1P	108	1.06	1.6E+05	1.3E+05	86%
Carnbee No. 1	CAR1P	105	1.24	4.0E+05	8.8E+05	217%
Charlottesville Nos. 1 and No. 2	CHR1P	107	0.92	1.6E+05	7.9E+04	49%
Craighall No. 1	CRG1P	207	0.98	1.2E+05	6.6E+05	542%
Diamond Estate Nos. 1 and 2	DIA1P	102	1.31	4.9E+05	9.6E+05	196%
Englishman's Bay No. 1	EBY1P	144	1.17	2.7E+05	1.3E+05	48%
Government Farms No. 6	GOV6P	249	0.86	1.1E+05	8.4E+05	774%
Kings Bay No. 1	KBY1P	13	0.86	2.5E+05	4.1E+04	17%
Mount Irvine Bay No. 1	IRV1P	253	1.38	3.7E+05	5.8E+04	16%
Sandy River No. 1	SYR1P	87	1.03	1.3E+05	3.6E+05	287%

AVL2P) and Campbelton (CAM1P). The Arnos Vale (AVL1P, AVL2P) well field must be capturing water that crosses topographic divides and/or is located along a regional groundwater flow path. The Adelphi (APH1P), Sandy River (SYR1P), and Bacolet (BAC1P, BAC3P, BAC5P) well fields, all located in the same watershed were also pumping at 143% of the recharge available within the topographic boundaries alone. Government Farms (GOV6P) and Campbelton (CAM1P) wells capture around 80% of the available recharge in the watershed. The watersheds where Craighall (CRG1P), Mount Irvine Bay (IRV1P), Belmont (BEL1P), Kings Bay (KBY1P), Charlottesville (CHR1P, CHR2P), and Bloody Bay (BB1P, BB2P) are located have the most recharge available that is not being captured.

In the analyses presented in the preceding, a conservative assumption is made that all water captured by existing well fields is delivered to the well from the area within topographic surface water divides. However, the sustained yields of certain well fields such as Arnos Vale (AVL1P, AVL2P) and Bacolet (BAC1P, BAC3P, BAC5P), both producing tremendous amounts of water relative to the size of the local topographic drainage, clearly indicated a source of additional recharge beyond what is available within local and upstream topographic basins (GRUs). In these situations, a mechanism must be invoked that allows groundwater to flow across topographic divides.

Figure 4 illustrates the correlation between highly productive pumping well subbasins and the interconnectivity of lineaments on the island. This suggests that there are preferential flow structures within the bedrock. The effect of the structures

on the hydrological routing of recharge was significant and shapes of the capture zones are controlled by the structural elements and the topography of the basins. This map represents a potential capture zone geometry of the well fields in a structurally controlled aquifer system. In the large east–west-trending structures in the southern part of the island, there is the possibility that well fields tap and capture water from up-gradient GRUs.

Stable isotope results

The water isotopic signatures of precipitation samples have a wide distribution, with $\delta^{18}\text{O}\text{-H}_2\text{O}$ values ranging from -6 to 2‰ and $\delta^2\text{H}\text{-H}_2\text{O}$ ranging from -35 to 10‰ . (Figure S7 of ESM1, Table S1 of ESM2). The recharge isotope signature for every precipitation station is more depleted than the annual weighted average. This is the case because the wet season precipitation is more isotopically depleted in the heavy isotopes than the dry season rainfall. Seven out of the 11 precipitation stations have recharge isotope signatures in a defined cluster with $\delta^{18}\text{O}\text{-H}_2\text{O}$ ranging from -3.25 to -2.5‰ and $\delta^2\text{H}\text{-H}_2\text{O}$ ranging from -14 to -8‰ . Wet and dry season groundwater samples also plot within the same cluster. There are four precipitation stations that fall outside of the general cluster that have no geographical characteristics in common besides low elevation. The absence of precipitation data from February to May does not affect possible recharge isotope signatures, as the water budget analysis predicts that there is nearly zero recharge on the island from February to May. The isotopic signature at each precipitation station

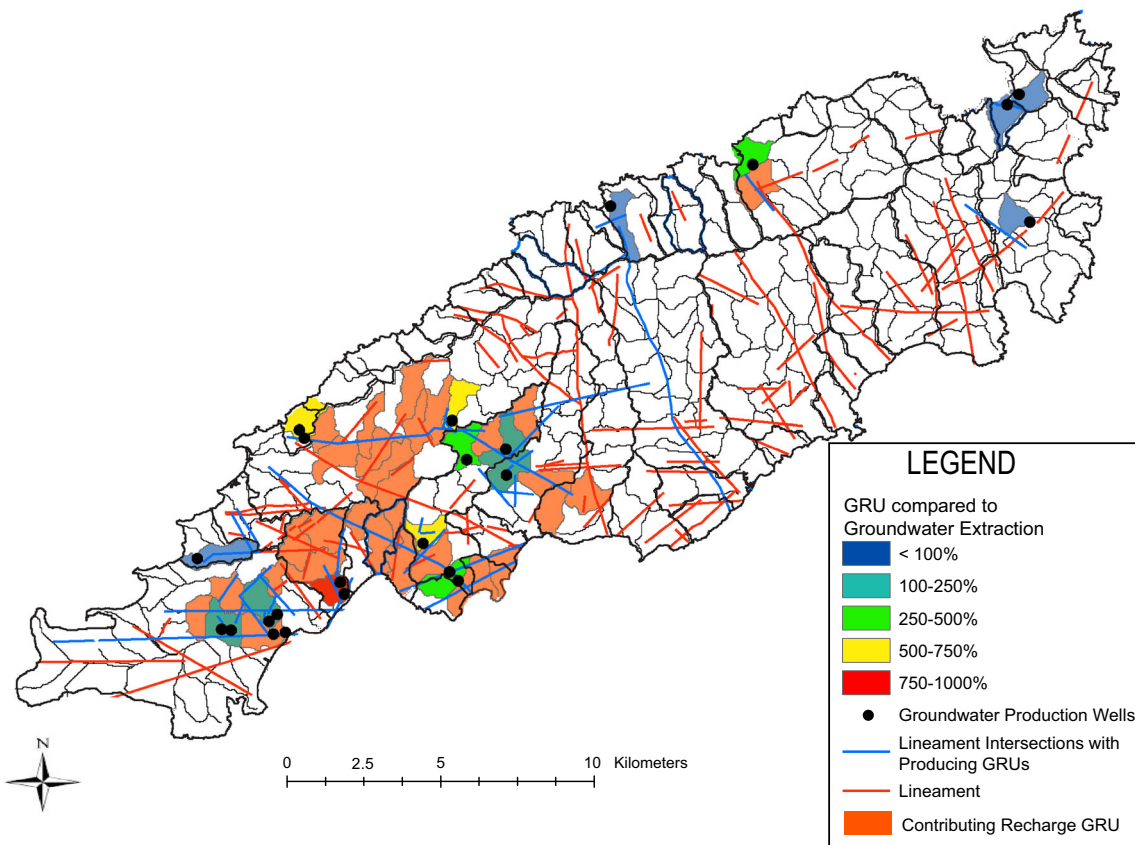


Fig. 4 Map illustrating the relationship of contributing groundwater recharge units (GRUs) subtracted from groundwater extraction contributions, in percentages

follows a distinct pattern over time, with $\delta^{18}\text{O}\text{-H}_2\text{O}$ levels becoming more depleted during the wet season, and then enriching during the dry season.

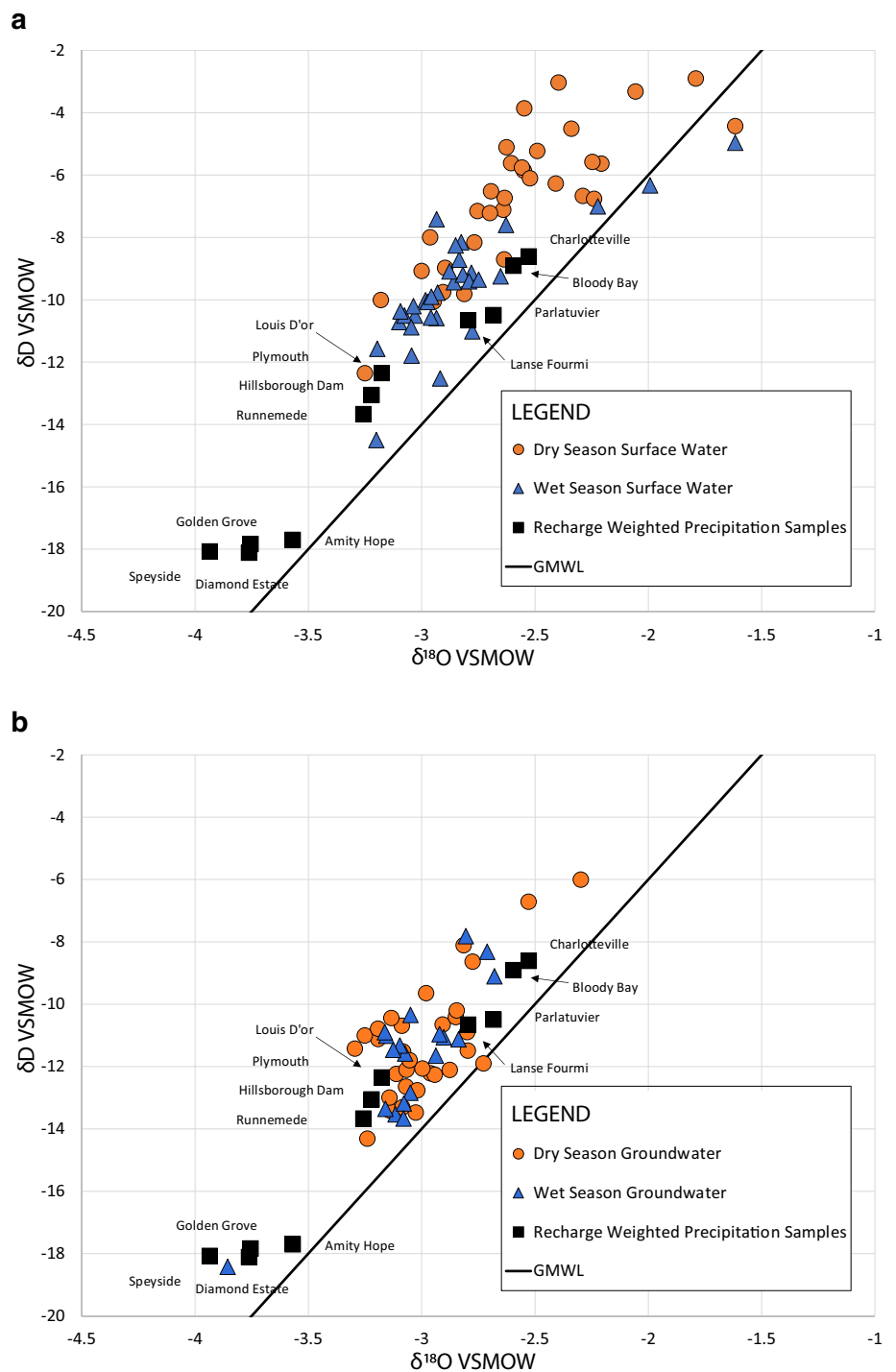
Stable isotope signatures of dry and wet season surface waters differ considerably from one another (Fig. 5a). Wet season surface waters plot similar to the groundwater signature, with $\delta^{18}\text{O}$ ranging between -3.5 and -2.5‰ , and $\delta^2\text{H}\text{-H}_2\text{O}$ values range from -14 to -8‰ . Dry season surface waters are enriched with heavier isotopes, with $\delta^{18}\text{O}\text{-H}_2\text{O}$ ranging between -3.5 and -1.5‰ , and $\delta^2\text{H}\text{-H}_2\text{O}$ values ranging from -13 to -2‰ . The pattern of enriched isotopes in the dry season and depleted isotopes in the wet season is observed in both precipitation and surface waters unlike the ground waters (Fig. 5a,b). The wet and dry season groundwater stable isotope signatures are similar to each other and have a distinct signature compared to the broad distribution of seasonal precipitation stable isotopes (Fig. 5b). The $\delta^{18}\text{O}\text{-H}_2\text{O}$ values for dry and wet season groundwater range between -3.5 and -2.5‰ , and $\delta^2\text{H}\text{-H}_2\text{O}$ values range from -14 to -8‰ .

Steady-state model capture zones and water budget

Steady-state simulations of groundwater flow on the island of Tobago are presented under pumping conditions from the

current installed borehole capacity. Initial homogeneous-isotropic simulations poorly matched observed hydraulic heads and dry-season stream discharge measurements. Fifteen different models were generated using hydraulic properties for map-scale geologic units and major structures and lineaments to find a suitable match (within 10% root-mean squared error) between hydraulic head measurements and dry-season stream discharge measurements. All models presented conserve mass within 0.01% of the total mass flux. The hydraulic conductivity distribution of the model with the lowest residual errors between simulated and observed heads and discharge values is presented in Fig. 6. Hydraulic conductivities vary from 0.01—low permeability to 80 m/day (small sand and gravel aquifers)—and were consistent with large-scale aquifer test results from the few datasets available. Specifically, the simulated hydraulic conductivity of the faults and lineaments in the model is consistent with hydraulic conductivities estimated from aquifer test results from wells targeting those structures. Simulated hydraulic heads for this model are shown in Fig. 7 and range from ~ 414 m asl to sea level. A comparison of observed hydraulic heads to simulated heads is presented in Fig. 8. The root-mean squared error for the mean observation wells is 8.27 m for all head observations (4.4 m for head measurements withheld during calibration

Fig. 5 **a** Groundwater and **b** surface water stable isotope sample results (δD vs $\delta^{18}O$ ‰) from 2014. The distinction between wet and dry seasons is made only based on the time of year the sample was collected



process) across the range of heads from 1 to 140 m asl. From the hydrologic analysis, the dry season stream discharge (assumed to be representative of groundwater discharge (baseflow) across all seasons, i.e. Boutt et al. (2001), is estimated to be 1.33 m³/s (Table 1) and the best-fit model generates 1.16 m³/s of groundwater discharge to streams (~86% of observed). The groundwater budget for this simulation in Table 3 shows the steady-state fluxes in and out of the island. Recharge dominates the water inputs to the island (94%) with

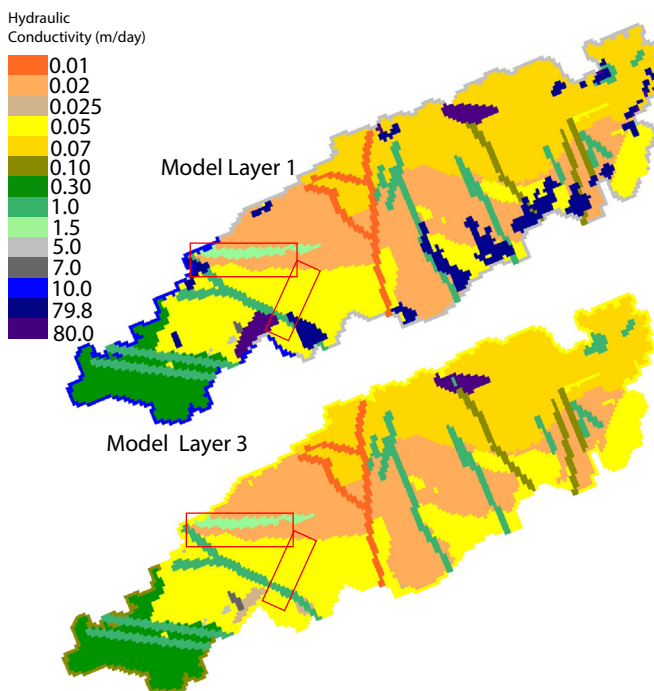
a minor (~6%) amount of induced stream leakage into the system. Groundwater flow to the ocean as submarine groundwater discharge dominates the outflow (64%), followed by stream baseflow (25%), and groundwater extraction from production wells (11%). The induced stream leakage is likely impacted by groundwater withdrawal and is confined to a small area of the southwest portion of the island. The magnitude of groundwater discharge to the coast is a very large portion of the budget and may be elevated slightly due to the

Table 3 Model derived groundwater steady-state budget for the island of Tobago

Water budget component	Flow in (m ³ /day)	Flow out (m ³ /day)	Flow in % (-)	Flow out % (-)
Ocean	0	2.53E+05	0%	64%
Production wells	0	4.03E+04	0%	10%
Recharge	3.70E+05	0	94%	0%
Stream leakage	2.30E+04	1.00E+05	6%	25%
Total	3.93E+05	3.93E+05	–	–

lack of the incorporation of small coastal stream systems in the model. However, given that the model comes close to matching the observed discharge of the major stream systems this effect is assumed to be minimal. The location of ground discharge to the coast is localized along the more permeable lineaments and through the hydraulically conductive sand and gravel deposits.

While a relationship between the water-table elevation and topography is present (Fig. 7), the highest hydraulic heads are not coincident with the highest topography on the island. Large stream systems (and their topographic influence) have a strong control on the patterns of the hydraulic heads. Four distinct groundwater mounds develop due to the combination of the recharge, lineament distribution, and topography that create distinct flow systems. The high groundwater mounds lie to the south (and off the axis) of the major watershed divides. The large lineament in the center of the island has significantly lower hydraulic conductivity than the rest of the units because it happens to intersect an area of high

**Fig. 6** Hydraulic conductivity distribution for the island-scale hydrogeologic model (m/day) for layers 1 and 3. The red rectangles are used to highlight which regions have the potential for interbasin flow

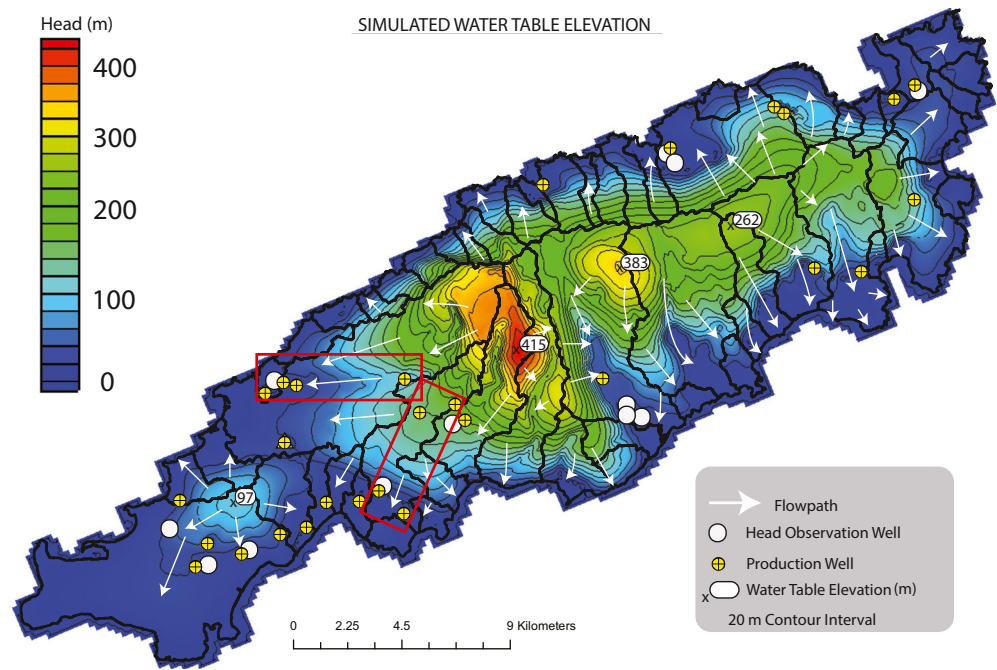
recharge (section ‘[Stable isotope results](#)’) and in models when the hydraulic conductivity of this lineament was of larger magnitude all of the water drained vertically downwards rather than distributing radially across the island. The position of this lineament relative to the zone of high recharge makes it a key determinant of how groundwater flows and how much of it flows to the rest of the island. The modeled capture zones (Fig. 9) for the island’s production wells are strongly influenced by both the presence of these lineaments and the locations of the groundwater mounds. The size of the capture zones is influenced by well production rates and the hydraulic conductivity distribution in the vicinity of the well. Consistent with the interpretation from Fig. 4 (contributing areas), the contributing zones to wells often extend beyond the local groundwater recharge unit and in some cases outside of the major island subcatchment (see red boxes in Figs. 6, 7, and 9). Because a single realization is used to generate path lines (and resulting capture zone interpretations), the exact position of the contributing areas is subject to uncertainty. The capture zones should not be interpreted as exact contributing areas of groundwater to production wells but reflect a general representation of possible contributing areas. Different realizations of hydraulic conductivity distributions will result in different spatial distributions of contributing areas—for example, the modification of hydraulic conductivity of the biotite-tonalite geologic unit (Fig. S8 of [ESM1](#)) has a large impact on the distribution of path lines and determination of the contributing area (uppermost red box in Fig. 9). Figure 10 is a modified version of the Snoke et al. 2001 geological map of Tobago’s cross section line B–B’. This figure represents a vertical dimension of this aquifer system. The area highlighted (upper red box) figure represents the connectivity between faults and fractures that allow groundwater to cross topographical boundaries, creating interbasin flow.

Discussion

Water budget, uncertainty, and limitations

The water budget for the island is based on a robust collection of precipitation data collected over the years 1976–2006. While focus here is on average hydro-climate conditions, inter-annual variability is present in the dataset and not

Fig. 7 Simulated water-table elevation for the steady-state groundwater flow model representing mean annual conditions. The red rectangles are used to highlight which regions have the potential for interbasin flow



incorporated into the assessments. Year to year precipitation variability is controlled by wet season precipitation and the length of the dry season resulting in 1 standard deviation (SD) of approximately 400 mm/year. Because groundwater recharge occurs predominantly in the wet season, large variations in wet season precipitation are likely going to lead to changes in net groundwater recharge. Spatially, the largest amount of uncertainty in the water budget comes from the high elevation locations on the island. It is assumed that

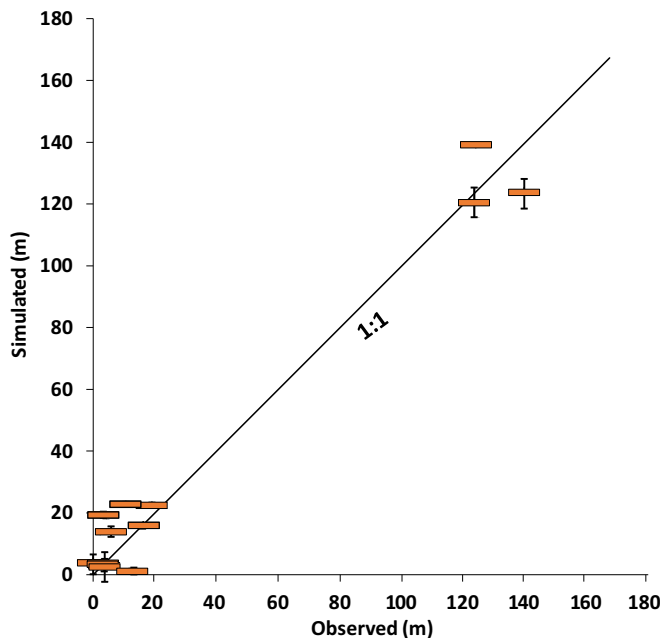


Fig. 8 Groundwater observed vs simulated heads (m) from the steady groundwater flow model. Error bars represent the range of observed water levels over the course of the monitoring period

extremely high rainfall rates occur at high elevations on the island during rainstorm events in the wet season, although incorporating these events into a multi-year precipitation map is unrealistic given the available data. A significant portion of precipitation in the 30-year isohyetal map (Fig. 4) is allocated to these higher elevation regions, despite the lack of empirical data available for this study. As a result, the 30-year isohyetal map predicts a high spatial intensity of rainfall in an area with high uncertainty. The likelihood of these extreme higher intensity events influencing recharge is low and the unrecorded high intensity precipitation as the events at high elevations are accompanied by equally and proportionally large unrecorded high intensity peaks in stream discharge.

Estimating streamflow discharge in the vegetated, high-gradient catchments of the island is challenging. The Trinidad and Tobago WASA-WRA collects dry season discharge measurements, which are used in this study, but wet season discharge remains relatively unconstrained. The approach here is to use high streamflow coefficients during the wet season, which has the impact of minimizing net groundwater recharge estimates. Because some fraction of dry season discharge is baseflow, the estimates minimize groundwater recharge by having more net discharge during dry season precipitation. Together these decisions provide groundwater recharge estimates that should be considered on the low side of possible scenarios.

Defining contributing areas in structurally complex aquifers

In homogenous isotropic unconsolidated aquifer systems, groundwater flow is dictated by climate/topography and

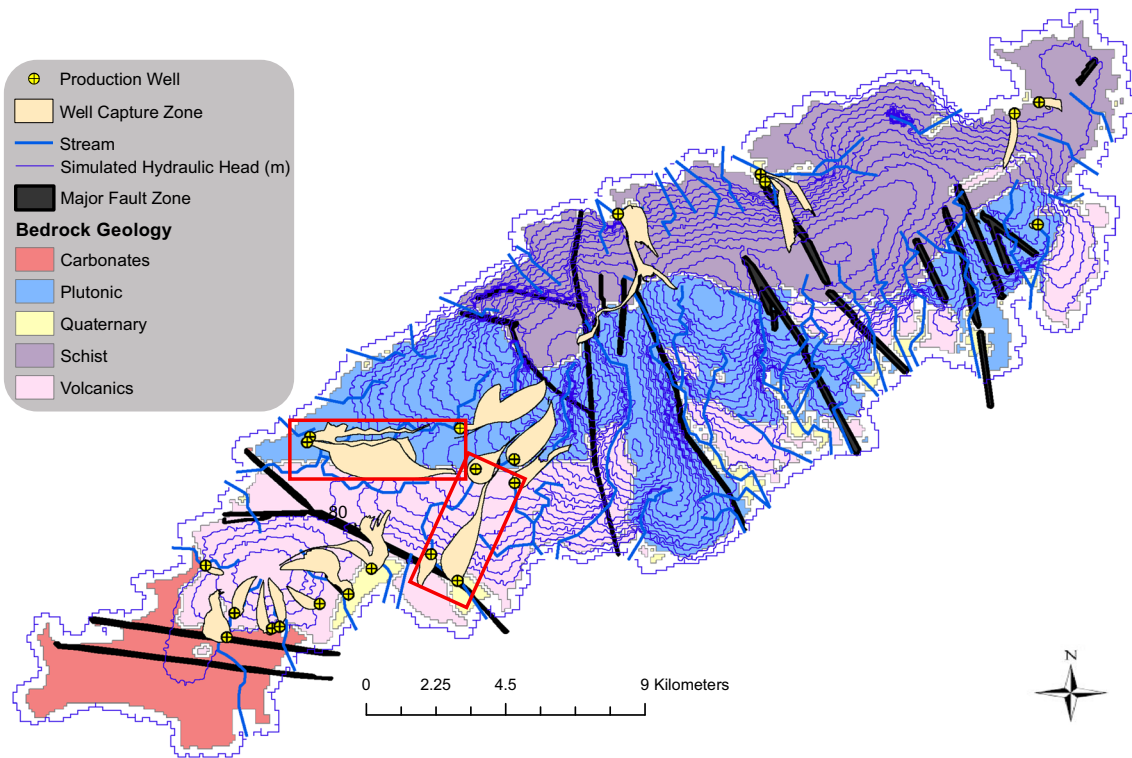


Fig. 9 Simulated production-well capture zones for the steady-state groundwater flow model. Delineated capture zones (red rectangles) are a strong function of the hydraulic conductivity distribution within the

model and represent approximate zones of contribution under steady-state pumping conditions

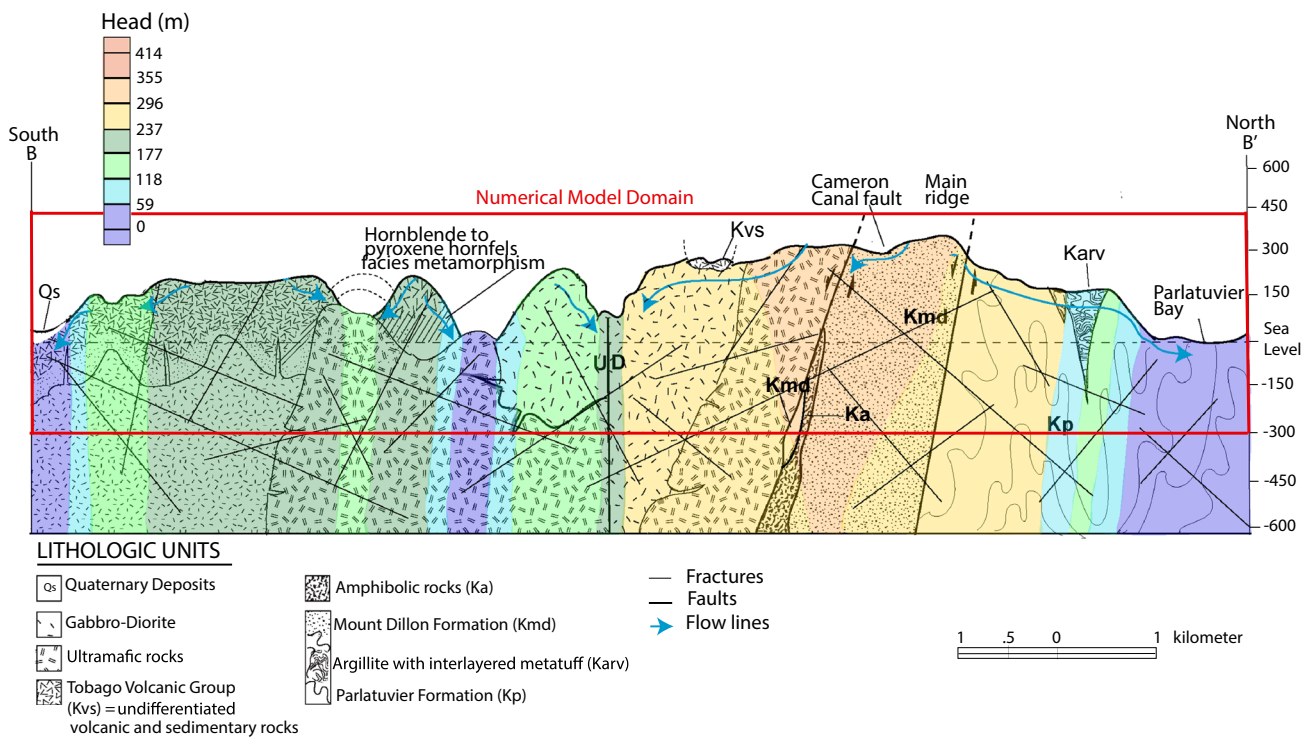


Fig. 10 Geologic cross-section along B–B' line (Fig. 2) showing the numerical model domain and simulated hydraulic heads. Schematized flow lines show the relationship between structures, topography, and groundwater flow

groundwater withdrawals are usually sourced from within the topographic watershed boundaries (Haitjema 1995; Haitjema and Mitchell-Bruker 2005; Gleeson et al. 2011). In crystalline bedrock aquifer systems that are highly faulted such as (Caine and Tomusiak 2003; Seaton and Burbey, 2005; Kim et al. 2003) and in Tobago, the tilted volcanic layers and layer bound fractures and faults create preferential groundwater flow paths. These faults allow for groundwater to flow from one topographic watershed to another, and transport large volumes of water from the highlands to the coast. Predicting contributing areas to groundwater wells in fractured rock aquifers is one of the most challenging aspects in fractured rock hydrogeology (Lyford et al. 2003; Hsieh and Shapiro 1996; Mabee et al. 1994; Seaton and Burbey 2005).

Two different approaches are presented to estimate the contributing areas of groundwater pumping in a structurally complex island-aquifer system ranging from simple to complex. The simple basin models take a water balance approach with no regard to the heterogeneous distribution of hydraulic properties (section ‘Contributing area to production well: hydrologic balance approach’). Potential preferential flow is included in an additional analysis and calculation (though still simplistic) in Fig. 4. Capture zones defined via a process-based groundwater flow model are the most sophisticated approach presented here (Fig. 9), although they still in some ways are limited by the equivalent porous media approach used in the model. The approach here shows a range of results that are the most robust given the scale of interest and data available. While the interest here is more focused on water supply sustainability, there are some drawbacks to this approach. Major assumptions regarding the scale and the nature of the structural features (i.e. which features are hydraulically important) is a key point. Additionally, the scale and resolution of the model presented here proposes issues with adequately resolving small-scale capture zones from pumping wells. For example, zones in the northeast of the island have small capture zones that cover less than numerical grid cells; therefore, the exact size and orientation is subject to high uncertainty.

Similarly, steady-state assumptions of hydrologic closure tend to maximize the size of the capture zones, as storage (under transient conditions) would result in more water being available closer to the extraction point. Analysis of water level data in bedrock pumping wells indicate seasonal changes in levels (suggesting water drawn from storage on an annual basis) but show no statistically significant declines in hydraulic head in 15+ years of records. These approaches are not likely to be as valid for issues dealing with contaminant transport, where more precise information regarding flow paths is needed. Nevertheless, the incorporation of fractured rock permeability and structures in the approach used here provides a way to conceptualize the flow system. Additionally, it is important to define the contributing areas of terrestrial

groundwater recharge to streams and submarine groundwater discharge for water supply managers to address questions regarding impacts of subsurface water withdrawals on sustainability of the aquifer system. Regardless, the process-based groundwater flow models incorporate all of the available hydrologic and hydrogeologic data and represent a robust approach to determine aquifer processes and sustainability.

Water isotope systematics

The results from the water budget suggest that groundwater recharge occurs in the wet season from June to December, with the majority of recharge occurring from September to December. Analysis of stable isotopes shows a temporal control on groundwater isotope signatures, supporting wet season recharge. This is evidenced by the wet-season precipitation and surface water bias in the groundwater isotopic compositions. The time series of $\delta^{18}\text{O}$ in precipitation shows that $\delta^{18}\text{O}$ decreases as the wet season approaches and begins to resemble the signature of groundwater. Groundwater isotope signatures are very similar in both wet and dry seasons. This suggests that the aquifer system has flow paths with residence times longer than 5 years (Kirchner 2016) and has large storage (because longer transit times allows mixing and equilibration of the seasonal precipitation isotopic signal). The majority of recharge signatures for precipitation stations (which were calculated using the estimates of monthly recharge) plot within the same range as groundwater signatures. There are four precipitation stations that have a more depleted signature than groundwater. The only similarities of these wells are that they are all located at lower elevations and are closer to the coast. Dry season surface water and dry season precipitation show a more enriched signature, originating from a different moisture source, which is not reflected in groundwater. Surface-water evaporative enrichment is not a likely explanation as the waters fall close to the meteoric water line. The culmination of these geochemical analyses supports that recharge occurs in the wet season, a finding also predicted by the water budget of this study.

Implications for groundwater sustainability

The monthly distribution of precipitation and potential evapotranspiration has implications for recharge and the timing of available water on the islands. The highest PET values coincide with the lowest precipitation values in April and May; during those periods AET is 40% of PET. During the highest rainfall month (November), PET is only moderate, leaving excess precipitation for streamflow and recharge. This seasonal fluctuation in PET and rainfall reflects the temporal availability of water on the island. As PET declines in the later months due to cooler temperatures, a greater amount of incoming precipitation is available to generate streamflow, as is

reflected in the discharge peaks measured at Tobago's four river flow measurement stations (Fig. S5 of [ESM1](#)) in November. The hydrological analysis of this study suggests that on average 21% of the incoming precipitation becomes groundwater recharge, primarily during the wet season. Existing production wells produce 11% of this water, or ~2.5% of the precipitation input. Groundwater flow path reconstruction suggests that a large percentage of this groundwater's ultimate fate is in submarine groundwater discharge, with the rest being captured from baseflow in the island's stream network. There are some areas such as the Courland river basin, where production wells have a larger impact on streamflow.

This study has established the important framework for the water budget on the island that allows water suppliers to make informed decisions regarding water usage and allocation. There is still uncertainty regarding the distribution of groundwater paths in bedrock, and physical process by which water infiltrates through the thick saprolite soils on the island. Future effort to utilize environmental tracers to conceptualize transit times in the island's fractured rock aquifer system will help confirm or refute the results of this study and reduce conceptualization-based uncertainty in the aquifer flow system. Together these data help form the basis by which the island can sustainably develop and maintain its water supply.

Conclusions

A hydrogeological study of groundwater recharge of the island of Tobago was conducted to provide a process-based understanding of the hydrologic and hydrogeologic conditions on the island. The groundwater storage on the island is almost entirely recharged during the wet season (May to November), amounting to 20% of total precipitation. The hydrological water budget analysis revealed that 11 out of 14 wells were producing more than their local groundwater recharge areas are capable of supplying, implying that substantial inter-basin flow within the island is occurring, as a result of the structural control on the hydraulic conductivity of the aquifer. Tobago's fractured rock groundwater aquifer system transports water from mountainous high elevation regions to the low elevation regions enabling fresh groundwater to be pumped below sea level from wells <1 km from the coast. The groundwater isotopic signatures do not vary seasonally, and show similar isotopic composition, suggesting an interconnected fractured bedrock aquifer. Simulations of mean annual conditions, with a steady-state groundwater flow model predict that not all groundwater recharge contributes to dry season streamflow discharge. Consequently, submarine groundwater discharge accounts for a significant amount

of the hydrologic budget. The model predicts that only 11% of recharge is currently utilized for groundwater extraction, and about 60% of recharge contributes to submarine groundwater discharge.

The results of this research revealed critical factors that affect the storage and capture of this aquifer's groundwater. It also distinguishes the highly productive regions which are favorable areas for future production well locations. The steady-state model presents a solid mean annual estimate of the contributing areas where production wells are located, as well as a water budget for this aquifer system. However, it can be improved by: applying transience to the steady-state model using the results of climate model projections of temperature and precipitation, the addition of lineament layers to further observe its effect on the large-scale fractures that are already in the model. Finally, the analysis of geochemical and environmental data should be incorporated in to reveal which regions of the island exhibits groundwater mixing.

Prior to this study, little was known about the recharge conditions or the magnitude of groundwater storage in the fractured bedrock aquifer of the island. The results of the study help define the amount and possible locations of water captured by currently installed groundwater wells on the island. The definition of the groundwater recharge zones has enabled the water authority to make decisions on future well placement and management. Given significant uncertainty in the modeled capture zones, effort should be placed in improving the understanding of the role of large-scale structures on the hydraulic conductivity distribution. Additional installation of monitoring wells outside of pumping regions would enable more refined hydraulic conductivity distributions in the model calibration process. Finally, the identification of significant submarine groundwater discharge in the subsurface water budget could be used as a way to guide future groundwater exploration. Currently, the installed well capacity on the island appears to be capturing mostly freshwater that is flowing out to sea through a subsurface flow path.

Supplementary Information The online version contains supplementary material available at <https://doi.org/10.1007/s10040-020-02289-6>.

Acknowledgements Danielle Hare and Mitchell Isaacson are thanked for contributing to field work and support for hydrological analyses. Access to CGIAR-CSI data from their website (Trabucco and Zomer 2019) which is used for the PET calculations is appreciated. Isotope data published in this report are available freely online in the Water isotopes Database (Bowen 2019) and in the supporting information. Detailed comments and suggestions from the associate editor greatly improved the manuscript.

Funding information The support from the Trinidad and Tobago Water and Sewage Authority (WASA) and the Water Resources Authority (WRA) made this work possible.

References

- Aitken T, Mann P, Escalona A, Christeson GL (2011) Evolution of the Grenada and Tobago basins and implications for arc migration. *Mar Pet Geol* 28(1):235–258. <https://doi.org/10.1016/j.marpetgeo.2009.10.003>
- Allen RG, Pereira LS, Raes D, Smith M (1998) Crop evapotranspiration: guidelines for computing crop requirements. Irrig Drain Pap no. 56, FAO, Rome. <https://doi.org/10.1016/j.eja.2010.12.001>
- Arenas AD (1983) Tropical storms in Central America and the Caribbean: characteristic rainfall and forecasting of flash floods. In: Hydrology of humid tropical regions with particular reference to the hydrologic effects of agriculture and forestry practice (Proc. of the Hamburg Symposium, August 1983). IAHS Publ. no. 140, pp 39–51
- Baban S, Ramsewak D, Canisius F (2009) Mapping and detecting land use/cover change in Tobago using remote sensing and GIS. *Caribbean J Earth Sci* 40:3–13
- Banerjee P, Singh VS, Singh A, Prasad RK, Rangarajan R (2012) Hydrochemical analysis to evaluate the seawater ingress in a small coral island of India. *Environ Monit Assess* 184(6):3929–3942. <https://doi.org/10.1007/s10661-011-2234-0>
- Banks EW, Simmons CT, Love AJ, Cranswick R, Werner AD, Bestland EA, Wood M, Wilson T (2009) Fractured bedrock and saprolite hydrogeologic controls on groundwater/surface-water interaction: a conceptual model (Australia). *Hydrogeol J* 17(8):1969–1989. <https://doi.org/10.1007/s10040-009-0490-7>
- Barton CA, Zoback MD, Moos D (1995) Fluid flow along potentially active faults in crystalline rock. *Geol* 23(8):683–686. [https://doi.org/10.1130/0091-7613\(1995\)023<0683:Ffapaf>2.3.Co;2](https://doi.org/10.1130/0091-7613(1995)023<0683:Ffapaf>2.3.Co;2)
- Bense VF, Gleeson T, Loveless SE, Bour O, Scibek J (2013) Fault zone hydrogeology. *Earth-Sci Rev* 127:171–192. <https://doi.org/10.1016/j.earscirev.2013.09.008>
- Biryukov D, Kuchuk FJ (2012) Transient pressure behavior of reservoirs with discrete conductive faults and fractures. *Transp Porous Media* 95(1):239–268. <https://doi.org/10.1007/s11242-012-0041-x>
- Boutt DF, Hyndman DW, Pijanowski BC, Long DT (2001) Identifying potential land use: derived solute sources to stream baseflow using ground water models and GIS. *Ground Water*. <https://doi.org/10.1111/j.1745-6584.2001.tb00348.x>
- Boutt DF, Diggins P, Mabee S (2010) A field study (Massachusetts, USA) of the factors controlling the depth of groundwater flow systems in crystalline fractured-rock terrain. *Hydrogeol J*. <https://doi.org/10.1007/s10040-010-0640-y>
- Bowen (2019) [Waterisotopes.org](https://waterisotopes.org), <https://wateriso.utah.edu/waterisotopes/>. Accessed November 10, 2020
- Brown SR, Bruhn RL (1998) Fluid permeability of deformable fracture networks. *J Geophys Res* 103(B2):2489–2500. <https://doi.org/10.1029/97JB03113>
- Buss HL, Sak PB, Webb SM, Brantley SL (2008) Weathering of the Rio Blanco quartz diorite, Luquillo Mountains, Puerto Rico: coupling oxidation, dissolution, and fracturing. *Geochim Cosmochim Acta* 72(18):4488–4507. <https://doi.org/10.1016/j.gca.2008.06.020>
- Buss HL, Mathur R, White AF, Brantley SL (2010) Phosphorus and iron cycling in deep saprolite, Luquillo Mountains, Puerto Rico. *Chem Geol* 269(1–2):52–61. <https://doi.org/10.1016/j.chemgeo.2009.08.001>
- Caine JS, Evans JP, Forster CB (1996) Fault zone architecture and permeability structure. *Geology* 24(11):1025–1028. [https://doi.org/10.1130/00917613\(1996\)024<1025:FZAAPS>2.3.CO;2](https://doi.org/10.1130/00917613(1996)024<1025:FZAAPS>2.3.CO;2)
- Caine JS, Tomasiak SRA (2003) Brittle structures and their role in controlling porosity and permeability in a complex Precambrian crystalline-rock aquifer system in the Colorado Rocky Mountain front range. *Bull Geol Soc Am*. <https://doi.org/10.1130/B25088.1>
- Charlier JB, Lachassagne P, Ladouche B, Cattani P, Moussa R, Voltz M (2011) Structure and hydrogeological functioning of an insular tropical humid andesitic volcanic watershed: a multi-disciplinary experimental approach. *J Hydrol* 398(3–4):155–170. <https://doi.org/10.1016/j.jhydrol.2010.10.006>
- Collins IIIWH, Easley DH (1999) Fresh-water lens formation in an unconfined barrier-island aquifer. *J Am Water Resour Assoc* 35(1):1–22
- Craig H (1961) Isotopic variations in meteoric waters. *Science*. <https://doi.org/10.1126/science.133.3465.1702>
- Daly C, Neilson RP, Phillips DL (1994) A statistical-topographic model for mapping climatological precipitation over mountainous terrain. *J Appl Meteorol* 33(2):140–158. [https://doi.org/10.1175/1520-0450\(1994\)033<0140:ASTMFM>2.0.CO;2](https://doi.org/10.1175/1520-0450(1994)033<0140:ASTMFM>2.0.CO;2)
- Davis SN, Turk LJ (1964) Optimum depth of wells in crystalline rocks. *Groundwater*. <https://doi.org/10.1111/j.1745-6584.1964.tb01750.x>
- Dingman SL (2002) Water in soils: infiltration and redistribution. In: *Physical hydrology*, 2nd edn. Prentice-Hall, Upper Saddle River, NJ, 646 pp
- Earnest E, Boutt D (2014) Investigating the role of hydromechanical coupling on flow and transport in shallow fractured-rock aquifers. *Hydrogeol J*. <https://doi.org/10.1007/s10040-014-1148-7>
- Ferguson G, Gleeson T (2012) Vulnerability of coastal aquifers to groundwater use and climate change. *Nat Clim Change* 2(5):342–345. <https://doi.org/10.1038/nclimate1413>
- Gleeson T, Marklund L, Smith L, Manning AH (2011) Classifying the water table at regional to continental scales. *Geophys Res Lett*. <https://doi.org/10.1029/2010GL046427>
- Government of the Republic of Trinidad and Tobago-Ministry of Public Utilities (2017) National Integrated Water Resource Management policy. Government of the Republic of Trinidad and Tobago, Port of Spain, 60 pp
- Gustafson G, Krásný J (1994) Crystalline rock aquifers: their occurrence, use and importance. *Appl Hydrogeol* 2(2):64–75. <https://doi.org/10.1007/s100400050051>
- Hamm SY, Cheong JY, Jang S, Jung CY, Kim BS (2005) Relationship between transmissivity and specific capacity in the volcanic aquifers of Jeju Island, Korea. *J Hydrol* 310(1–4):111–121. <https://doi.org/10.1016/j.jhydrol.2004.12.006>
- Haitjema HM (1995) On the residence time distribution in idealized ground watersheds. *J Hydrol*. [https://doi.org/10.1016/0022-1694\(95\)02732-5](https://doi.org/10.1016/0022-1694(95)02732-5)
- Haitjema HM, Mitchell-Bruker S (2005) Are water tables a subdued replica of the topography? *Ground Water*. <https://doi.org/10.1111/j.1745-6584.2005.00090.x>
- Hargreaves GH, Allen RG (2003) History and evaluation of Hargreaves evapotranspiration equation. *J Irrig Drain Eng*. [https://doi.org/10.1061/\(ASCE\)0733-9437\(2003\)129:1\(53](https://doi.org/10.1061/(ASCE)0733-9437(2003)129:1(53)
- Heilweil VM, Healy RW, Harris RN (2012) Noble gases and coupled heat/fluid flow modeling for evaluating hydrogeologic conditions of volcanic island aquifers. *J Hydrol* 464–465:309–327. <https://doi.org/10.1016/j.jhydrol.2012.07.019>
- Herrera DA, Ault TR, Fasullo JT, Coats SJ, Carrillo CM, Cook BI, Williams AP (2018) Exacerbation of the 2013–2016 Pan-Caribbean drought by anthropogenic warming. *Geophys Res Lett*. <https://doi.org/10.1029/2018GL079408>
- Holding S, Allen DM, Foster S, Hsieh A, Larocque I, Klassen J, Pelt SC Van (2016) Groundwater vulnerability on small islands. *Nat Clim Chang*. <https://doi.org/10.1038/nclimate3128>
- Hsieh PA, Shapiro AM (1996) Hydraulic characteristics of fractured bedrock underlying the use well field at the Mirror Lake site, Grafton County, New Hampshire. US Geological Survey Toxic Substances Hydrology Program—Proceedings of the Technical Meeting, Colorado Springs, CO, September 1996
- Karmalkar AV, Taylor MA, Campbell J, Stephenson T, New M, Centella A, Benzanilla A, Charlerly J (2013) A review of observed and

- projected changes in climate for the islands in the Caribbean. *Atmosfera* 26(2):283–309. [https://doi.org/10.1016/S0187-6236\(13\)71076-2](https://doi.org/10.1016/S0187-6236(13)71076-2)
- Karnauskas KB, Donnelly JP, Anchukaitis KJ (2016) Future freshwater stress for island populations. *Nat Clim Chang* 6(7):720–725. <https://doi.org/10.1038/nclimate2987>
- Kim Y, Lee KS, Koh DC, Lee DH, Lee SG, Park WB, Koh GW, Woo NC (2003) Hydrogeochemical and isotopic evidence of groundwater salinization in a coastal aquifer: a case study in Jeju volcanic island, Korea. *J Hydrol* 270(3–4):282–294. [https://doi.org/10.1016/S0022-1694\(02\)00307-4](https://doi.org/10.1016/S0022-1694(02)00307-4)
- Kirchner JW (2016) Aggregation in environmental systems, part 1: seasonal tracer cycles quantify young water fractions, but not mean transit times, in spatially heterogeneous catchments. *Hydrol Earth Syst Sci*. <https://doi.org/10.5194/hess-20-279-2016>
- Koh DC, Niel Plummer L, Kip Solomon D, Busenberg E, Kim YJ, Chang HW (2006) Application of environmental tracers to mixing, evolution, and nitrate contamination of ground water in Jeju Island, Korea. *J Hydrol*. <https://doi.org/10.1016/j.jhydrol.2005.11.021>
- Kretzschmar R, Robarge WP, Amoozegar A (1994) Filter efficiency of three saprolites for natural clay and iron oxide colloids. *Environ Sci Technol* 28(11):1907–1915. <https://doi.org/10.1021/es00060a022>
- Lyford BFP, Carlson CS, Hansen BP (2003) Delineation of water sources for public-supply wells in three fractured-bedrock aquifer systems in Massachusetts. United States Geological Survey Water-Resources Investigations Report
- Mabee SB, Hardcastle KC, Wise DU (1994) A method of collecting and analyzing lineaments for regional-scale fractured-bedrock aquifer studies. *Ground Water* 32(6):884–894
- Manda AK, Mabee SB, Boutt DF, Cooke ML (2013) A method of estimating bulk potential permeability in fractured-rock aquifers using field-derived fracture data and type curves. *Hydrogeol J* 21(2):357–369. <https://doi.org/10.1007/s10040-012-0919-2>
- Mimura N, Nurse L, McLean RF, Agard J, Briguglio L, Lefale P, Payet R, Sem G (2007) Climate Change 2007: impacts, adaptation and vulnerability—contribution of Working Group II to the fourth assessment report of the Intergovernmental Panel on Climate Change. <https://doi.org/10.1256/004316502320517344>
- Min KB, Jing L, Stephansson O (2004) Determining the equivalent permeability tensor for fractured rock masses using a stochastic REV approach: method and application to the field data from Sellafeld, UK. *Hydrogeol J* 12(5):497–510. <https://doi.org/10.1007/s10040-004-0331-7>
- Mogaji KA, Omosuyi GO, Olayanju GM (2011) Groundwater system evaluation and protective capacity of overburden material at Ile-Oluji, southwestern Nigeria. *J Geol Mining Res* 3:294–304
- Morin RH, Savage WZ (2003) Effects of crustal stresses on fluid transport in fractured rock: case studies from northeastern and southwestern USA. *Hydrogeol J* 11(1):100–112. <https://doi.org/10.1007/s10040-002-0235-3>
- Niswonger RG, Panday S, Ibaraki M (2011) MODFLOW-NWT, a Newton formulation for MODFLOW-2005: US Geol Surv Tech Methods 6-A37
- Öhman J, Niemi A, Tsang CF (2005) A regional-scale particle-tracking method for nonstationary fractured media. *Water Resour Res* 41(3):1–16. <https://doi.org/10.1029/2004WR003498>
- Pyrak-Nolte LJ, Morris JP (2000) Single fractures under normal stress: the relation between fracture specific stiffness and fluid flow. *Int J Rock Mech Min Sci* 37(1–2):245–262. [https://doi.org/10.1016/S1365-1609\(99\)00104-5](https://doi.org/10.1016/S1365-1609(99)00104-5)
- Penna D, Stenni B, Šanda M, Wrede S, Bogaard TA, Michelini M, Fischer BMC, Gobbi A, Mantese N, Zuecco G, Borga M, Bonazza M, Sobotková M, Čejková B, Wassenaar LI (2012) Technical note: evaluation of between-sample memory effects in the analysis of $\delta^2\text{H}$ and $\delta^{18}\text{O}$ of water samples measured by laser spectroscopes. *Hydrol Earth Syst Sci*. <https://doi.org/10.5194/hess-16-3925-2012>
- Pett-Ridge JC, Derry LA, Kurtz AC (2009) Sr isotopes as a tracer of weathering processes and dust inputs in a tropical granitoid watershed, Luquillo Mountains, Puerto Rico. *Geochim Cosmochim Acta* 73(1):25–43. <https://doi.org/10.1016/j.gca.2008.09.032>
- Robinson M, Beven KJ (1983) The effect of mole drainage on the hydrological response of a swelling clay soil. *J Hydrol* 64(1–4):205–223. [https://doi.org/10.1016/0022-1694\(83\)90069-0](https://doi.org/10.1016/0022-1694(83)90069-0)
- Seaton WJ, Burbey TJ (2005) Influence of ancient thrust faults on the hydrogeology of the Blue Ridge Province. *Ground Water*. <https://doi.org/10.1111/j.1745-6584.2005.0026.x>
- Schneider JC, Kruse SE (2003) A comparison of controls on freshwater lens morphology of small carbonate and siliciclastic islands: examples from barrier islands in Florida, USA. *J Hydrol* 284(1–4):253–269. <https://doi.org/10.1016/j.jhydrol.2003.08.002>
- Snoke AW, Rowe DW, Yule JD, Wadge G (2001) Petrologic and structural history of Tobago, West Indies: a fragment accreted Mesozoic oceanic arc of the southern Caribbean. <https://doi.org/10.1130/0-8137-2354-x.1>
- Speed RC, Smith-Horowitz PL, Perch-Nielsen KVS, Saunders JB, Sanfilippo AB (1993) Southern Lesser Antilles Arc Platform: pre-late Miocene stratigraphy, structure, and tectonic evolution. *Geol Soc Am* 277. <https://doi.org/10.1130/SPE277-p1>
- Speed RC, Smith-Horowitz PL (1998) The Tobago terrane. *Int Geol Rev* 40(9):805–830. <https://doi.org/10.1080/00206819809465240>
- Stringfield VT, Rapp JR, Anders RB (1979) Effects of karst and geologic structure on the circulation of water and permeability in carbonate aquifers. *Dev Water Sci*. [https://doi.org/10.1016/S0167-5648\(09\)70023-1](https://doi.org/10.1016/S0167-5648(09)70023-1)
- Trabucco A, Zomer R (2019) Global Aridity Index and Potential Evapotranspiration (ET₀) Climate database, vol 2. figshare. Fileset. <https://doi.org/10.6084/m9.figshare.7504448.v3>
- UNESCO (1986) Final report. In: First Workshop on the Hydrogeological Atlas of the Caribbean Islands, Santo Domingo, Dominican Republic, 7–10 October 1986. UNESCO/ROSTLAC, Montevideo, Uruguay, 229 pp
- Williams AJ, Crossey LJ, Karlstrom KE, Newell D, Person M, Woolsey E (2013) Hydrogeochemistry of the Middle Rio Grande aquifer system: fluid mixing and salinization of the Rio Grande due to fault inputs. *Chem Geol* 351:281–298. <https://doi.org/10.1016/j.chemgeo.2013.05.029>
- Zomer RJ, Trabucco A, Bossio DA, Verchot LV (2008) Climate change mitigation: a spatial analysis of global land suitability for clean development mechanism afforestation and reforestation. *Agric Ecosyst Environ* 126(1–2):67–80. <https://doi.org/10.1016/j.agee.2008.01.014>

Publisher's note Springer Nature remains neutral with regard to jurisdictional claims in published maps and institutional affiliations.